Sustainable Food Technology

ROYAL SOCIETY OF CHEMISTRY

PAPER

View Article Online
View Journal | View Issue

Cite this: *Sustainable Food Technol.*, 2026, 4, 752

PLA/starch bi-layer films reinforced with rice straw cellulose nanofibers and functionalized with organosolv–lignin nanoparticles and grapefruit bioactives for shelf life extension of green grapes

Makdud Islam, *[a] Akhouri Sanjay Kumar Sinha [b] and Kamlesh Prasad *[a]

The transition toward sustainable food packaging demands biodegradable composites with multifunctional performance. In this study, polylactic acid (PLA)/starch bi-layer composites were developed by reinforcing the PLA layer with succinic anhydride-modified cellulose nanofibers (SACNFs) from rice straw and functionalizing the starch layer with modified lignin nanoparticles (MLNPs) and/or grapefruit flavedo extract (GFE). The addition of 2 wt% MLNPs enhanced tensile strength by 25.3%, while GFE increased flexibility without significant loss in strength. Hybrid MLNPs + GFE films exhibited notable barrier improvements, reducing water vapor permeability and oxygen permeability by 16.5% and 39.3%, respectively. Structural (FE-SEM, XRD) and spectroscopic (FTIR, UV-Vis) analyses confirmed compact morphology, good interfacial compatibility, and strong UV-blocking ability (<9.7% transmittance at 250–300 nm). The active films demonstrated high antioxidant potential and antimicrobial activity against *Staphylococcus aureus* and *Pseudomonas aeruginosa*, attributed to synergistic effects of MLNPs and phenolic compounds from GFE. Enhanced thermal stability was also observed in MLNP-containing composites. Importantly, packaging trials with fresh green grapes revealed that the developed film (MLNPs + GFE) effectively reduced weight loss (17.1 ± 1.2%), delayed browning (0.84 ± 0.09), and extended the shelf life up to 18 days under refrigerated storage, significantly outperforming unpackaged and LDPE-packed grapes. Overall, these results highlight that PLA/starch bi-layer films functionalized with biomass-derived nanofillers and natural bioactives are a promising route for sustainable active packaging and shelf life extension of perishable fruits such as green grapes.

Received 5th September 2025
Accepted 5th November 2025

DOI: 10.1039/d5fb00561b

rsc.li/susfoodtech

Sustainability spotlight

This work advances sustainable food packaging by transforming rice straw and citrus peel two abundant agro-industrial residues into value-added components for multifunctional PLA/starch bi-layer films. Incorporation of cellulose nanofibers, organosolv–lignin nanoparticles, and grapefruit bioactives enhanced mechanical, water vapor barrier, UV barrier, antibacterial, antioxidant properties while reducing dependence on petroleum-based plastics. Importantly, packaging trials with green grapes demonstrated reduced weight loss, delayed browning, and extended shelf life up to 18 days under refrigeration, outperforming conventional LDPE films. By integrating waste valorization with improved preservation of perishable fruits, this study contributes to circular economy principles, reduction of plastic waste, and mitigation of food loss, aligning with sustainable food technology goals.

1 Introduction

Although petroleum-based plastics remain prevalent in food packaging and allied sectors, their use poses significant environmental challenges, including resource depletion and persistent non-biodegradable waste. In response, there has been a growing demand, particularly in the food and pharmaceutical industries, for sustainable, eco-friendly materials that fulfil modern packaging requirements.[1] In this regard, bioplastics synthesized from bio-based polymers are a potential alternative to petroleum-based polymers. Despite biopolymers having some limitations in terms of mechanical performance, thermal stability, and barrier properties, extensive research has focused on improving these attributes to match the performance of conventional petrochemical plastics.[2,3] Consequently, among the different bio-based polymers, poly(lactic) acid (PLA) stands out as one of the most promising biopolymers that are made from sustainable resources like sugarcane and maize starch due to its numerous advantages.[4] It is biodegradable, renewable, and biocompatible, with FDA approval for direct contact with biological fluids. Additionally, PLA offers

[a]*Department of Food Engineering and Technology, Sant Longowal Institute of Engineering and Technology, Punjab, India. E-mail: makubkv96@gmail.com; profkprasad@gmail.com*

[b]*Department of Chemical Engineering, Sant Longowal Institute of Engineering and Technology, Punjab, India*

high mechanical strength and an excellent water vapor barrier comparable to petroleum-based plastics like polyethylene terephthalate (PET) and polystyrene (PS). However, despite these benefits, PLA-based films have drawbacks such as being extremely brittle, with less elongation at break (<10%), poor barrier qualities (such as oxygen), and insufficient UV protection, all of which are critical for prolonging the shelf life of perishable goods.[5] One potential solution to address these limitations is to combine it with other biopolymers that provide complementary characteristics. In this regard, starch is a suitable choice due to its high oxygen barrier properties, low cost, wide availability, and as well as easy ability to produce extensible films.[6] Nevertheless, starch films are extremely water-sensitive, have a low tensile strength, and a weak water vapor barrier capability.[7] In this regard, a bilayer design for PLA and starch was employed to overcome phase incompatibility often observed in composites, improve interlayer adhesion, maximize the efficiency of incorporated additives, and more closely mimic the structure of practical multilayer packaging systems.[8] However, there have been few studies into the obtaining of PLA-starch bilayer films.[9,10] Wang *et al.* (2024) characterized PLA/starch bi-layer produced by casting with varying polymer ratios and observed that at the ratio of PLA50/starch50, these bilayers demonstrated lower water vapor permeability and improved mechanical performance compared to starch films.[11] Since starch and PLA possess complementary properties regarding barrier capacity and mechanical performance, combining them in a bilayer structure could provide suitable materials for food packaging. PLA offers an effective barrier against water vapor, while starch is efficient in blocking oxygen. Moreover, an increasing amount of food in stores is packaged in advanced multilayer plastic films, which provide better long-term preservation compared to monolayer structures. Similarly, integrating nanoparticles and bioactive compounds into PLA and starch layers could result in an active, biodegradable food packaging material with enhanced functional properties.[12,13] Since natural antimicrobial compounds are rather expensive, bi-layer films are suggested as a way to help lower the amount of these compounds needed in films. The active compounds are only required for the second thin layer, which forms the surface that will come into contact with the food. The incorporation of nanocellulose from agro-biomass at a lower percentage (1 wt%) into the polymer matrix can enhance mechanical strength, reduce gas permeability, and improve polymer functionality due to its high aspect ratio.[14] Meanwhile, lignin nanoparticles extracted from lignocellulosic biomass provide a high barrier, mechanical and UV-blocking, and antioxidant and anti-microbial properties, making it valuable for advanced biopolymer films.[3,15] On the other hand, grapefruit flavedo extract (GFE), abundant in phenolics and flavonoids, possesses potential antioxidant and antimicrobial properties, making it a valuable addition to act as a protective function of packaging films. In parallel, the incorporation of GFE with bioactive properties into polymer matrices has been explored as an effective means to impart antioxidant and antimicrobial functionalities to the material.[2,16,17] Consequently, developing biodegradable and eco-friendly polymer composites from renewable agricultural residues, such as rice straw and grapefruit byproducts, supports both sustainable material design and the goals of a circular bioeconomy. This strategy is in line with recent advances in sustainable bio-based nanocomposites, where the incorporation of natural extracts and eco-friendly fillers has been shown to enhance material performance while minimizing environmental impact.[18–20] It is hypothesized that functionalizing the starch layer with organosolv lignin nanoparticles (MLNPs) and/or grapefruit peel extract (GFE) would synergistically enhance the performance of PLA/starch bi-layer films. Specifically, (i) MLNPs are expected to improve mechanical strength, UV-shielding, thermal stability, and barrier properties; (ii) GFE is anticipated to provide antioxidant, antimicrobial, and plasticizing effects; and (iii) their combined incorporation (F3) is expected to yield balanced improvements, extending the shelf life of green grapes. These hypotheses were experimentally tested and statistically validated against the control sample (C) ($p < 0.05$). A schematic representation of the designed PLA/starch bi-layer films reinforced with SACNFs and functionalized with MLNPs and GFE, along with their expected functional properties, is shown in Fig. 1.

To the best of our knowledge, no study focuses on the development of rice straw (RS) SA_CNFs reinforced PLA/starch bi-layer films added with MLNPs from RS rice straw and GFE from grapefruit flavedo waste added to the starch layer. The current study deals with the development and detailed characterization of bi-layer films based on PLA/potato starch, in which SA_CNFs from RS were reinforced in the PLA layer, and MLNPs and/or GFE are added to the second starch layer. The details characterization, such as microstructure (FE-SEM), and physical properties of the different bi-layer films were analyzed, as well as thermal properties (TGA, DSC), crystallinity (XRD), barrier properties (OP, WVTR), anti-microbial and antioxidant properties, and molecular interaction through FT-IR analysis. Additionally, the fabricated active films were practically evaluated in grape packaging, where weight loss and browning degree of the packaged grapes were measured to assess their effectiveness for green packaging applications.

2 Materials and methods

2.1 Materials

The succinic anhydride-modified cellulose nanofiber (SACNFs) and lignin (organosolv-treated) solution from rice straw used for this study were acquired from our previous work.[21] Grapefruit

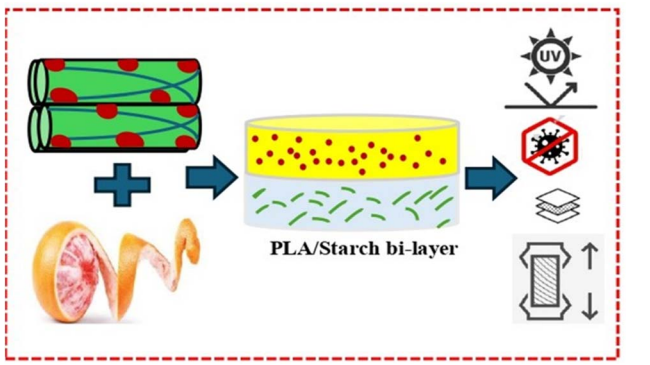

Fig. 1 Schematic illustration of PLA/starch bi-layer films with SACNFs, MLNPs, and GFE for active food packaging.

was purchased from the local market of Chandigarh, and potato starch (Cat. No. 06120) was obtained from Lova Chemie Pvt. Ltd, Mumbai, India with a high purity (>99%), amylose (~20–25%), and moisture (<15%) was used for this research. Chemicals such as succinic anhydride (SA), DPPH, ABTS, acetate buffer, TPTZ solution, and ferric chloride hexahydrate, potassium persulfate, sodium nitrite, aluminum chloride, sodium hypophosphite, sodium hydroxide, Folin–Ciocaltue solution, sodium carbonate, dichloromethane are analytical grade and supplied by Himedia Pvt (Mumbai). Poly(lactic acid) (PLA), marketed as Luminy® LX175 and manufactured by Total Corbion, is a highly viscous, amorphous, and transparent white pellets. It contains approximately 4% D-lactic acid and has a molecular weight of 163 000 g mol^{-1} and it has a density of 1.24 g cm^{-3} and a melt flow index (MFI) of 6 g/10 min (measured at 210 °C under a 2.16 kg load).

2.2 Synthesis and surface modification of lignin nanoparticles (MLNPs)

Lignin nanoparticles were synthesized through a pH-induced precipitation method, followed by a previous method with slight modifications.[22] After the extraction of cellulose, the organosolv-treated black liquor solution (Lignin) was transferred to a 300 mL beaker under constant stirring for 1 h to achieve a uniform suspension, and subsequently, 0.25 M hydrochloric acid (HCL) was added dropwise (3 drops per min) to have a pH value of 3.07. After 6 h, the mixture was transferred into tubes and filtered with distilled water (DL) until a neutral pH was achieved. Again, the mixture was subjected to centrifugation (900*g*, 15 min), filtered through Whatman filter paper, and ultrasonicated in an ultrasonic probe sonicator (Q500, Newtown, USA) at 40% amplitude for 30 min and freeze-dried to obtain powdered LNPs for further functionalization. To modify the LNPs, LNPs suspension was mixed with a 5 wt% citric acid solution and a 1 wt% sodium hypophosphite (NaH_2PO_4) as a catalyst. The mixture was then kept in a vacuum oven (0.6 bar) for 2 h, and then it was left to stand at RT for 12 h. The chemical modification started to operate after excess water was removed in an oven at 60 °C and cured for 4 h at 130 °C.[23] To eliminate residual citric acid, NaH_2PO_4, and unstable byproducts, the solid phase was redissolved in water, centrifuged three times, and dialyzed against DL until reaching neutral pH. Afterward, the suspension underwent ultrasonic treatment before being evenly distributed into water. Finally, the modified LNPs (MLNPs) were obtained as a powder from a freeze-dryer (−50 °C, 0.12 mbar).

2.3 Extraction of grapefruit (*Citrus paradisi*) flavedo extract (GFE)

The ethanolic extracts from grapefruit flavedo were obtained using an optimized ultrasonic extraction method.[24] Ultrasonic-assisted extraction was carried out using grapefruit flavedo powder (2 g) in a 48 9% ethanolic solution with an ultrasonic amplitude of 40% and a sonication time of 13 min in an ultrasonic probe sonicator (Q500, Newtown, USA). Following the completion of the sonication procedure, the sample was centrifuged at 500*g* for 10 min and allowed to cool to room temperature (RT) using a cold-water bath (0–4 °C). Ultimately, supernatants were filtered through a 0.45 nm nylon membrane into a 50 mL falcon tube and stored at 4 °C for further analysis. The flavedo extracts were placed in a Petri dish and kept in a vacuum drier overnight to evaporate the solvent from the Petri dish. Finally, a known ethanolic solution of GFE was then made by weighing the flavedo extract amount on a weighing balance. The ethanolic GFE solution was stored for further use in a refrigerator.

2.4 Fabrication of PLA_SACNFs/starch bi-layer films added with MLNPs and GFE

PLA and modified CNFs (SA_CNFs) bio-nanocomposite films were fabricated *via* modified solvent-casting.[25] In brief, PLA (5 g) pellets were blended into the dichloromethane solution (100 mL) and mixed vigorously using a magnetic stirrer (≈400 rpm) at 45 °C for 6 h. On the other side, dichloromethane solution was mixed with 1 wt% SA_CNFs and constantly swirled (≈400 rpm) for 8 h. After that, a probe sonicator at 40% amplitude (Q500, Newtown, USA) was used to sonicate this mixture for 30 min at RT. In addition, SA_CNFs (1 wt%) solutions were added to the pre-prepared PLA solution, and after 15 min of stirring, it was again sonicated for 30 min. Lastly, the resulting suspension (≈20–25 mL) was cast onto a 90 mm glass Petri dish and vacuum-dried at 50 °C to constant weight. Meanwhile, 4 g of potato starch was dispersed in DL and heated to 80–90 °C under continuous stirring until full gelatinization occurred. Cool the gelatinized starch solution to RT and add 30% glycerol to the starch solution. Afterward, disperse the pre-synthesized and 2 wt% surface-modified lignin nanoparticles (MLNPs) into the starch solution under vigorous stirring. Again, add 5 wt% grapefruit flavedo extracts (GFE) and continue stirring to ensure homogeneity. Once the PLA_SACNFs film was completely dried, the homogeneous starch mixture (≈12–15 mL) containing pure starch, MLNPs, GFE, or MLNPs + GFE was gently poured onto the pre-dried PLA_SACNFs layer according to the formulation protocol described in Table 1. The bi-layer films were then dried at 45 °C (30–40% RH) until complete solvent removal (approximately 12–18 h). After drying, the films were carefully peeled from the casting substrate and conditioned in a desiccator for at least 24 h prior to characterization. As this work extends our previous study, where the incorporation of 1 wt% SACNFs in the PLA matrix provided the highest tensile (26.54 MPa) and barrier properties (4.85 g mm per day per m^2 per kPa). Based on these results, the PLA + 1 wt% SACNFs layer was selected as the constant structural base, while the starch layer was modified with MLNPs and GFE to examine their effects on film functionality. Monolayer PLA or starch films were not included, as the aim was to investigate starch-layer functionalization over an optimized PLA substrate.

2.5 Film characterization

2.5.1 Structural and molecular interaction analysis

2.5.1.1 Fourier transform infrared spectroscopy (FT-IR) analysis. PLA_SACNFs/starch bi-layer films were subjected to FT-IR

Table 1 Experimental design of bi-layer films[a]

Sample ID	PLA layer composition	Starch layer composition	Description
C	PLA + 1 wt% SACNFs	Native starch	Control (no additives)
F1	PLA + 1 wt% SACNFs	Starch + 2 wt% MLNPs	MLNPs added to starch layer
F2	PLA + 1 wt% SACNFs	Starch + 5 wt% GFE	GFE added to starch layer
F3	PLA + 1 wt% SACNFs	Starch + 2 wt% MLNPs + 5 wt% GFE	MLNPs and GFE added to starch layer

[a] C: PLA_SACNFs/starch, F1: PLA_SACNFs/starch_2MLNPs, F2: PLA_SACNFs/starch_5GFE, F3: PLA_SACNFs/starch_2MLNPs_5GFE.

analysis using a previous methodology.[26] In a nutshell, 40–45 mg of film was cut into rectangular pieces and placed within the sample chamber. 64 scans of an interferogram were made using FT-IR (PerkinElmer, L1600300 Spectrum TWO LiTa, UK) with a scanning range of 4000–600 cm^{-1} and a resolution of ± 4 cm^{-1}.

2.5.1.2 X-ray diffraction (XRD) analysis. The X-ray diffraction pattern of bi-layer films was analyzed according to the method described by ref. 27. The analysis was performed using an X-ray diffractometer (Almelo, Netherlands) equipped with a Cu/Kα radiation source ($\lambda = 1.548$ Å). The films were scanned over an angular range of 5° to 40° (2θ) at a scanning rate of 0.5° min^{-1}.

2.5.1.3 FESEM analysis. The morphology of the bi-layer films was analyzed using a field emission scanning electron microscope (FE-SEM, JEOL, JSM 840, Japan). To avoid electrostatic charging, the samples were fixed onto aluminum stubs with conductive tape and sputter-coated with a thin gold layer. Observations were conducted at an accelerating voltage of 5 kV.

2.5.2 Thickness and mechanical properties. Film thickness was determined using a micrometer (Alton M820-25, China) with a precision of 0.01 mm at nine different points. The mechanical properties of the film samples, including tensile strength (TS), elongation at break (EAB,%), and Young's modulus (YM), were assessed using a texture analyzer (Stable Micro Systems, Surrey, UK) following ASTM D882-10 standards.[28] To measure each sample, a sample dimension of 60 mm × 20 mm was cut from it and added to the texture analyzer at a distance of 40 mm. During the measurement process, a speed limit of 1 mm s^{-1} was applied. For every sample, an average of five samples was measured. TS, EAB (%), and YM of the samples were measured using the following eqn (1)–(3)

$$\mathrm{TS(MPa)} = \frac{F}{X} \quad (1)$$

$$\mathrm{EAB}(\%) = \frac{\Delta L}{L_o} \times 100 \quad (2)$$

$$\mathrm{YM(MPa)} = \frac{\mathrm{TS}}{\mathrm{EAB}} \quad (3)$$

where F: maximum stretching strength (N), X: area of the film (mm^2), ΔL: elongated lengths (mm), and L_o: original length (mm).

2.5.3 Moisture content (MC), film solubility (FS), and film swelling ratio (SR). The MC of the films was estimated using the AOAC method.[29] FS was ascertained gravimetrically following a previous method with minor modification.[30] The film SR was calculated using a previously established procedure with slight changes.[31] The detailed procedures are described in Text S1.

2.5.4 Contact angle measurements. The contact angle of composite films was measured using a contact angle measurement system (Data Physics OCA 20, Germany) based on a previous methodology by with slight modifications.[32] The details methodology of the contact angle measurement is presented in the Text S1.

2.5.5 Water vapor permeability (WVP) and oxygen permeability (OP). WVP was determined gravimetrically using the desiccant method, followed by ASTM E96-00 with a minor modification.[33] In this method, the glass bottles containing anhydrous calcium chloride were sealed with films with a radius of 2 cm using paraffin wax. A desiccator with saturated sodium chloride solution was used to maintain a relative humidity (RH) of 75%. The weight of the cups was recorded every 24 h, and WVP was reported using the eqn (4)

$$\mathrm{WVP} = \frac{W \times x}{t \times A \times \Delta P} \quad (4)$$

where W: change in the weight of the glass bottles (g), x: thickness of the film (m), t: time (day), A: area of the film (m^2), and ΔP: saturated vapor pressure (Pa) at RT.

The bi-layer film's oxygen transmission rate (OTR) was measured following the ASTM (2004) protocol.[34] In this procedure, film samples with a diameter of 15 cm were securely mounted over the aperture of a diffusion chamber. Nitrogen gas (98% concentration) was introduced on one side, while oxygen (21% concentration) was applied on the opposite side. The tests were performed under 25 °C, 1 atm pressure, and 50% RH. Finally, calculate the OP value from the obtained OTR values by using the following eqn (5)

$$\mathrm{OP} = \frac{\mathrm{OTR} \times t}{\Delta P} \quad (5)$$

where OTR: oxygen transmission rate, t: material thickness, and ΔP: partial pressure difference of oxygen across the material.

2.5.6 Color parameters and opacity. The color parameters of the film, including L^*, a^*, and b^* measured using a Hunter colorimeter (model D25, Hunter Associates Laboratory Inc., USA) against a white plate background. The detailed methods and formulas for the color change, whiteness index (WI), and film opacity are presented in Text S1.

2.5.7 Ultraviolet and visible light transmission. UV-visible light barrier properties of the films were assessed using a UV-Vis spectrophotometer (PerkinElmer, Waltham, USA) according to the procedure reported by a previous method.[35] In this

process, film strips with dimensions of 10.0 cm × 1.5 cm were firmly positioned in the cuvette holder of the spectrophotometer to ensure that the light beam reached their surfaces directly. The initial layer of the film was in direct contact with the cuvette while the transmittance was measured in triplicate over the 200–800 nm wavelength range.

2.5.8 Total phenolic content (TPC) and total flavonoid content (TFC). The TPC of the bi-layer films was quantified using a previous methodology with slight modifications,[36] while the TFC was determined following a previous procedure.[37] Detailed methodologies are provided in Text S1.

2.5.9 Antioxidant activity (AA). The radical scavenging activity (RSA) of the films was evaluated using the 2,2-diphenyl-1-picrylhydrazyl (DPPH) assay, following the method described in a previously published method.[38] Antioxidant activity was further assessed using the 2,2-azinobis(3-ethylbenzothiazoline-6-sulfonate) (ABTS) radical cation decolorization assay with minor modifications.[24] The ferric-reducing antioxidant power (FRAP) was measured following the method reported by Eskandarabadi *et al.* (2019) with minor adjustments.[39] The detailed methodologies are provided in Text S1.

2.5.10 Anti-microbial activity. The anti-microbial activity of the bi-layer films was assessed using a previous method with a few modifications.[40] In brief, 20 mL of plant count agar (0.0175 g mL^{-1}, pH 5.5) was prepared, sterilized, and poured into Petri dishes. Around 50 μL of a 48 h incubated nutrient broth culture (8 mg mL^{-1}) containing active strains of *Pseudomonas aeruginosa* (MTCC 1366) and *Staphylococcus aureus* (MTCC 96) was added to the solidified agar surface. The test films were then put into a circular well that was made in the middle of each plate and had a diameter of 10 mm. The plates were incubated for 24 h for *S. aureus* and 48 h for *P. aeruginosa* at 37 °C. The zone of inhibition was identified after incubation by measuring the diameter of the clear zone surrounding the film in millimeters. Films without additives were used as controls.

2.5.11 Differential scanning calorimetry (DSC) analysis. The films were analyzed using DSC (Perki-nElmer, DSC 4000, UK). Approximately 2.5 mg of each film sample was sealed in an aluminum pan and subjected to a heating cycle from 25 °C to 100 °C at a rate of 10 °C min^{-1}. The samples were then cooled back to 25 °C and reheated to 200 °C at the same rate. Throughout the analysis, a constant nitrogen flow of 60 mL min^{-1} was maintained. The glass transition temperature (T_g), melting temperature (T_m), and enthalpy of fusion (H_f) were determined from the second heating cycle.

2.5.12 Thermogravimetric analysis (TGA). The thermal behavior of the PLA bi-layer films was examined by TGA (Perkin Elmer-TGA 4000) analysis. A 70 μL aluminum pan was used to hold approximately 50 mg of the sample. Thermogravimetric analysis (TGA) was performed over a temperature range of 30–500 °C, with a heating rate of 10 °C min^{-1} and a nitrogen gas flow rate of 20 mL min^{-1}. The TGA and derivative thermogravimetric (DTG) curves were used to evaluate the sample's weight loss, residual mass, and thermal stability.

2.6 Functional efficiency of active films

Fresh, healthy green grapes free from microbial contamination and mechanical damage were carefully selected and sorted for uniformity in size, color, and ripeness. The grapes were washed with distilled water, weighed, and packaged using different materials, including LDPE films, bi-layer active films. Unpacked grapes served as a control. Packaging trials were conducted under two conditions: storage at 3 °C for 0, 4, 8, 12, 16, and 18 days, assess the performance of AMC active films. The freshness and shelf life extension of grapes under different packaging systems were monitored throughout the storage period.

2.6.1 Weight loss analysis. Weight loss was determined by recording the grape weights on the 1st, 4th, 8th,12th, 16th, and 18th days of storage using a LEADZM electronic balance. The reduction in weight over time was used as an indicator of weight loss, which was calculated using eqn (6):

$$\text{Weight loss}(\%) = \frac{W_o - W_f}{W_o} \times 100 \quad (6)$$

where, W_o is the initial weight, W_f is the final weight.

2.6.2 Antibrowning analysis. The browning degree of grapes was evaluated using the extinction value method after 18 days of storage.[41] A grape solution of 20% (w/v) was prepared by homogenizing the sample with cold steamed water. The absorbance of this solution was measured at 410 nm, and the browning degree was expressed as A_{410} (absorbance at 410 nm).

2.7 Statistical analysis

All experiments used three independently prepared film batches per formulation (biological replicates) with multiple technical replicates: thickness (nine points per sheet × three sheets), mechanical tests (five strips, ASTM D882), UV-Vis (three strips), barrier properties (three samples), and antioxidant/antimicrobial assays (triplicat). For grape packaging trials, each treatment (unpackaged, LDPE, control, F1–F3) included three trays under identical refrigerated conditions, with randomized and rotated positions, and analyses performed blind. Data are expressed as mean ± SD and analyzed by ANOVA with film batch as a random effect, followed by Duncan's Multiple Range Test ($p < 0.05$). Normality and homogeneity were verified, and non-parametric tests applied when necessary.

3 Results and discussion

3.1 Structural and molecular interaction analysis

3.1.1 FT-IR analysis. FT-IR spectra were performed to identify the possible interaction among the different polymers (PLA, starch) and additives (SACNFs, MLNPs, GFE). FT-IR spectra of C, F1, F2, and F3 bi-layer films are shown in Fig. 2a. The FT-IR spectra of PLA_SACNFs/starch bi-layer films show the O–H stretching peak at around 3373 ± 4 cm^{-1}, due to intermolecular and intramolecular hydrogen bonding of starch and SA-modified CNFs reinforced into the PLA matrix. Upon incorporation of bio-additives, a noticeable shift in the O–H stretching peak toward lower wavenumbers was observed, indicating compositional changes and stronger hydrogen-

bonding interactions induced by MLNPs and GFE.[42] Specifically, the O–H stretching bands appeared at 3311 ± 4 cm^{-1} for F1 (MLNPs), 3357 ± 4 cm^{-1} for F2 (GFE), and 3349 ± 4 cm^{-1} for F3 (MLNPs + GFE), suggesting enhanced hydrogen bonding and intermolecular associations between hydroxyl groups of starch and the phenolic or carboxylic groups of the additives. Quantitative integration of the FT-IR spectra was carried out for the O–H (3200–3600 cm^{-1}) and C=O (1700–1760 cm^{-1}) regions after baseline correction. The resulting O–H/C=O area ratio increased from 1.08 ± 0.05 (control) to 1.25 ± 0.04 (F1), 1.18 ± 0.03 (F2), and 1.30 ± 0.05 (F3). The higher ratios confirm an increased contribution of hydrogen-bonded hydroxyl groups in the modified films, consistent with stronger interfacial interactions and improved molecular compatibility between the PLA and starch layers. The absorption peaks near 1450 ± 4 cm^{-1}, and 2918 ± 4 cm^{-1}, suggest the CH_3 bending and stretching of the PLA layer from the PLA_SACNFs/starch bi-layer films. However, the peak intensity at around 1181–1078 ± 4 cm^{-1}, suggests the C–O stretching of PLA and bands at around 1150-900 ± 4 cm^{-1}, corresponding to the starch polysaccharide backbone. The peak intensity at around 2918 ± 4 cm^{-1}, due to the C–H (CH_2–) stretching is slightly shifted to 2928 ± 4 cm^{-1}, 2964 ± 4 cm^{-1}, and 2923 ± 4 cm^{-1}, in the case of F1, F2, and F3 bi-layer films, respectively, which may be due to the intermolecular interactions and structural rearrangements induced by the incorporation of bio-additives. Moreover, a strong absorption peak at around 1745 ± 4 cm^{-1}, indicating ester carbonyl groups due to the PLA films.[14] However, when MLNPs and GFE were incorporated into the starch films, new absorption peaks appeared at 1649 ± 4 cm^{-1}, and 1035 ± 4 cm^{-1}, corresponding to C–C and C–O stretching vibrations of phenolic and aromatic compounds present in the additives. These spectral shifts suggest strong intermolecular interactions and structural integration without major chemical changes in the PLA or starch backbone. A similar observation was reported in another study, where lignin nano-encapsulated anthocyanins incorporated into PVA–PEG-based packaging films exhibited comparable peaks.[43] A subtle shoulder at 1750 cm^{-1} in F1–F3 films was attributed to carbonyl stretching of ester and carboxylic groups from MLNPs and GFE. Interactions between GFE's carbonyls and starch may also cause slight shifts. The observed shifts in this region suggest possible interactions such as hydrogen bonding or esterification between the hydroxyl groups of starch and GFE_MLNPs. These hydrogen bonds, formed between starch and MLNPs or GFE, likely influence the microenvironment of absorbed water, leading to changes in the C=O stretching peak, either by shifting its position or decreasing its intensity. Such modifications imply enhanced water resistance and reduced moisture sensitivity in the film. Similarly, Kaya *et al.* (2018) reported changes in FT-IR peak intensity and position in chitosan-based films containing *Pistacia terebinthus* extracts, indicating strong intermolecular interactions between the extract and the film matrix.[44] In the present study, FT-IR analysis confirmed no significant alterations in the functional groups of the PLA_SACNFs/starch bi-layer films, suggesting that the chemical structure remained intact despite the incorporation of bio-additives. The minor shifts in peak intensity and position observed can be attributed to physical interactions, such as hydrogen bonding and van der Waals forces, between the bio-additives and the polymer matrix.[45]

3.1.2 XRD analysis. The X-ray diffraction (XRD) patterns of the control sample (C) and modified films (F1–F3) are shown in Fig. 2b. In the control bi-layer film (PLA_SACNFs/starch), characteristic diffraction peaks of PLA are observed at approximately 16.8° ± 0.1°, 19.4° ± 0.1°, and 22.0° ± 0.1° (2θ), which correspond to its semi-crystalline nature. Similarly, potato starch exhibits diffraction peaks within the 15–23° (2θ) range, indicative of its B-type crystalline structure associated with amylose and amylopectin. These peaks in the control film are primarily attributed to the PLA layer.[46] However, variations in peak

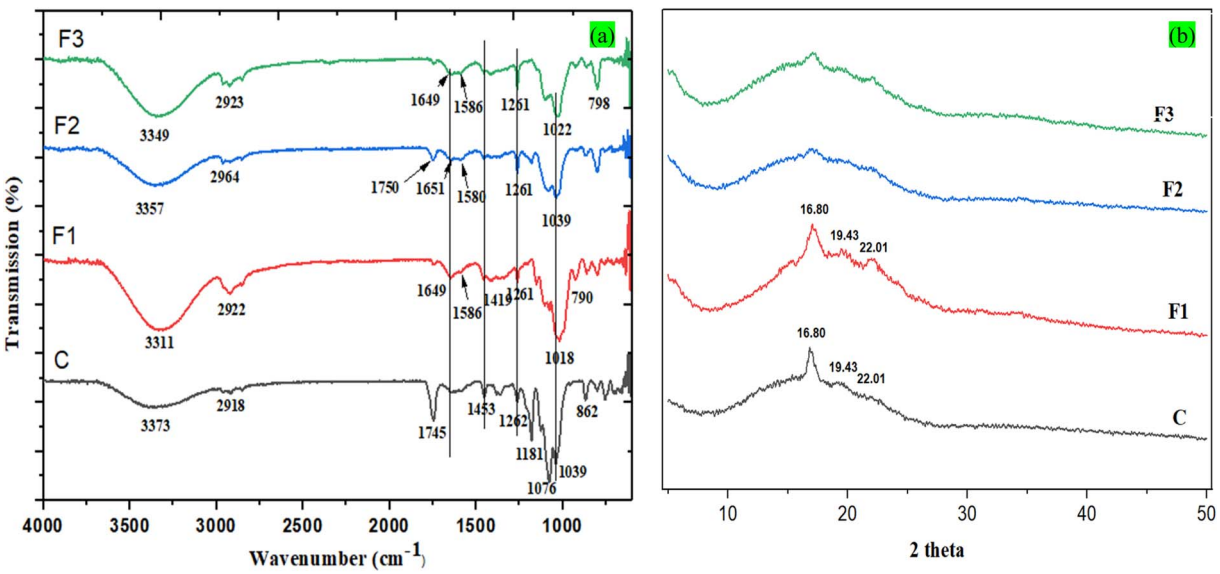

Fig. 2 FT-IR spectroscopy (a) and XRD pattern (b) of bi-layer films.

intensity and slight broadening suggest possible interactions or structural modifications due to the incorporation of bio-additives such as MLNPs and GFE in the starch layer. However, the crystallinity index (CrI, %) of the films increased from 35.5 ± 1.5% (C) to 39.5% (F1) due to the nucleating effect of MLNPs, which facilitated the formation and growth of ordered crystalline regions, particularly within starch's B-type crystalline structure.[47,48] This enhancement was reflected by the sharper and more intense diffraction peaks at 16.80°, 19.43°, and 22.01° (2θ), indicating improved molecular ordering. In contrast, the addition of GFE (F2) decreased CrI to 29.5%, accompanied by broader and less intense peaks that shifted slightly to lower angles. This reduction suggests amorphous caused by polyphenolic compounds such as flavonoids and phenolic acids, which interfere with starch chain packing and act as mild as crosslinkers and plasticizers.[49] Similar effects have been reported by Jha (2020), where the incorporation of grapefruit seed extract (GSE) into corn starch/chitosan/clay films caused peak shifts and reduced crystallinity due to polyphenol–polymer interactions.[50] The combined effect of MLNPs and GFE in the film (F3) exhibited an intermediate crystallinity of 31.5%, with moderately broadened peaks and a diffuse hump between 10–30° (2θ), reflecting a balanced interplay between crystalline reinforcement by MLNPs and amorphous flexibility introduced by GFE. The diminished intensity of PLA peaks at 16.80° and 19.43° further indicates partial disruption of ordered domains and increased interfacial compatibility between PLA and starch layers. Overall, these results confirm that MLNPs and GFE collectively modulate the crystalline–amorphous balance through interfacial interactions, as further supported by FT-IR evidence of enhanced hydrogen bonding within the bi-layer films. Although direct studies on the combined effects of MLNPs and GFE on starch crystallinity are limited, however, their individual effects support the synergistic effects of MLNPs and GFE.

3.1.3 FESEM analysis. Fig. 3 shows the FE-SEM morphology of the PLA_SACNFs/starch bi-layer films added with MLNPs and GFE bio-additives. The control film (C) exhibits a standard PLA/starch bi-layer structure. The control film (C) which shows the native starch, exhibited a smooth and somewhat visibly rough surface on the starch layer. The incorporation of modified lignin nanoparticles (MLNPs) enhances the structural uniformity of the starch layer. Due to their good compatibility, these nanoparticles function as reinforcing agents, promoting the formation of a continuous matrix. This morphological behavior aligns with previous findings on starch-based films containing lignin nanoparticles.[42] Additionally, the inclusion of grapefruit flavedo extract (GFE) may contribute to a smoother and more homogeneous surface without visible cracks, likely due to increased polymer chain mobility. In the F3 samples, FE-SEM images are expected to a more compact microstructure and improved dispersion of lignin nanoparticles. The starch layer in these samples likely exhibits enhanced cohesion, and stronger internal interactions. Similar structural characteristics have been reported in other studies.[51,52]

3.2 Film thickness and mechanical properties

Table 2 demonstrates that the thickness of the bi-layer films varied significantly based on their layer compositions, particularly the layer with the addition of starch, MLNPs, and GFE. The control sample (C) exhibited the lowest thickness of about ~0.09 mm, and F3 (PLA_SACNFs/starch_2MLNPS_5GFE) showed the highest thickness of around ~0.112 mm, while the incorporation of additional functional components, such as MLNPs and GFE, into the starch layer led to a noticeable increase in film thickness. This, combined with the observed improvements in barrier properties, may suggest a more compact or cohesive structure, likely resulting from synergistic interactions between the matrix and the additives. Comparable trends have been observed in prior studies, where biopolymer-based films with blended or layered formulations showed increased thickness due to enhanced material deposition and interaction among constituents.[6,53]

The mechanical properties of the bi-layer films, including tensile strength (TS), elongation at break (EAB, %), and elastic modulus (YM), were also affected by the incorporation of bio-additives such as MLNPs and GFE in the second (starch) layer, as presented in Table 2. This study is a continuation of our previous work, which revealed that incorporating 1 wt% SACNFs into PLA films achieved an optimal balance between tensile strength and barrier properties. Therefore, this optimized PLA composition was selected as the base layer (1st layer) for the bi-layer film formulation. A similar improvement in strength properties at low nanocellulose (0.5–1 wt%) loadings have also been reported for PLA-based films.[54] Moreover, the addition of MLNPs enhanced the TS by 25.30% and increased the YM from 0.810 to 0.850 GPa compared to the control films (C). Additionally, a slight increment in EAB (%) from 4.74% to 5.40% for the addition of MLNPs in the starch layer (F1). This improvement in TS and YM is attributed to the uniform distribution of MLNPs within the starch matrix, facilitating hydrogen bonding and achieving strong compatibility and physical reinforcement. Similar enhancement in TS and YM has been documented for starch-based films reinforced with lignin nanoparticles, highlighting their effectiveness in improving the mechanical properties of biopolymer composite films.[42] Conversely, the inclusion of GFE in the second layer resulted in a slight reduction in TS and YM (from 29.72 MPa to ~27.80 MPa and 0.810 GPa to 0.799 GPa, respectively). Additionally, the EAB increased from 4.74% to 6.40%, indicating a plasticizing effect induced by this antimicrobial agent. The incorporation of GFE acted as a plasticizer in potato starch-based films, leading to a noticeable reduction in tensile strength due to weakened starch–starch interaction forces.[55] However, the combined effect of MLNPs and GFE on the starch layer minor reduction in TS by ~4%, and EAB (%) from 4.74% to 5.70%, and EM from 0.810 to 0.795 GPa, which values are slightly higher than the F2 sample but lower than F1 and the control sample. These results suggested a balancing effect between physical reinforcement with MLNPs and GFE-induced plasticization, where the GFE plasticization effect dominates over MLNP's reinforcement. A similar observation was detected for the bi-layer gelatin-based

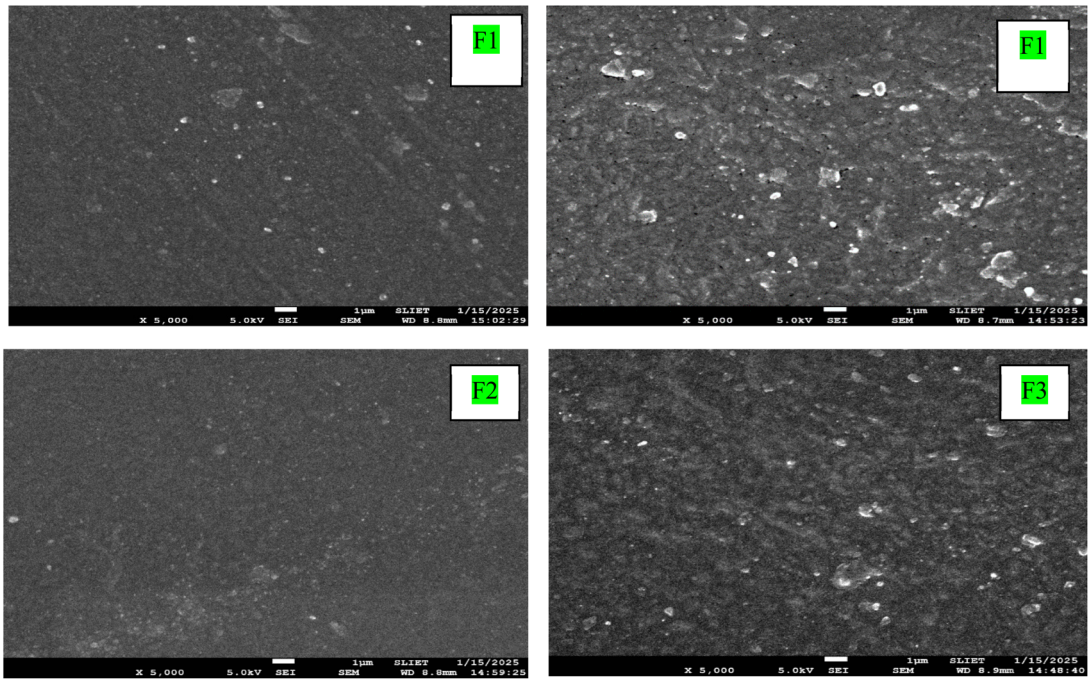

Fig. 3 FE-SEM morphology of bi-layer films.

films added with "Pitanga" leaf extract and nisin on the second layer.[13]

3.3 MC, FS, and SR

Water resistance is a key factor in packaging materials, ensuring durability and preserving food freshness for a longer shelf life. Therefore, understanding the MC, SR, and FS of these materials is important when designing packaging films.[56] The data from Tables 2 and 3 indicate that the incorporation of MLNPs and GFE in the starch layer of bi-layer films contributed to enhanced water resistance by reducing the MC, FS, and SR of the films. The control film (C) exhibited high MC, FS, and SR of 10.30%, 45.12%, and 72.15%, respectively, which is the characteristic of native starch films due to their strong hydrophilic nature. However, the addition of MLNPs (F1) led to significant reductions ($p < 0.05$) in MC, FS, and SR by 28%, 55.05%, and 55.44%, respectively. The hydrophobic interactions and cross-linking between lignin nanoparticles and starch molecules probably cause the decrease in solubility seen with MLNPs inclusion (F1). Previous studies also demonstrated that lignin-based fillers enhance hydrophobicity by forming a compact polymer network, limiting water penetration.[42] Similarly, the incorporation of GFE (F2) also contributed to lowering the MC, FS, and SR by 18.05%, 43.59%, and 43.53%, respectively, due to the presence of polyphenolic compounds and pectin, which interact with starch chains to enhance structural integrity and moisture resistance. A similar kind of result was observed for starch-based bio-plastic film added with citrus lemon peel ethanol extracts.[6] However, with regards to the MC, FS, and SR of the films, the synergistic effect of MLNPs and GFE (F3) further enhanced water resistance by reducing the MC, FS, and SR by 1.65, 2.43, and 2.41 times, respectively, by reinforcing the fillers through hydrogen bonding and hydrophobic interactions. However, there is no significant difference ($p < 0.05$) compared to the F1 bi-layer films. This is consistent with other research that reported that the combined effect of melanin nanoparticles and grapefruit seed extract on the pectin/agar blended films improves water resistance by reducing the water solubility.[45]

3.4 Contact angle measurements

Fig. 4 presents the water contact angle (WCA) measurements of the PLA_SACNFs/starch bilayer films, surface (starch-layer)

Table 2 Thickness, moisture, tensile strength (TS), Young modulus (YM), and elongation at break (EAB, %) values of bi-layer films[a]

Sample ID	Thickness (mm)	Moisture (%)	TS (MPa)	EAB (%)	YM (GPa)
C	0.090 ± 0.003^{b}	10.30 ± 0.85^{a}	29.72 ± 1.54^{b}	4.74 ± 0.35^{b}	0.810 ± 0.07^{a}
F1	0.105 ± 0.005^{a}	7.13 ± 0.74^{c}	37.24 ± 1.75^{a}	5.40 ± 0.45^{b}	0.85 ± 0.06^{a}
F2	0.095 ± 0.004^{b}	9.26 ± 0.95^{b}	27.80 ± 1.45^{c}	6.74 ± 0.55^{a}	0.799 ± 0.05^{a}
F3	0.112 ± 0.006^{a}	6.84 ± 0.65^{c}	28.50 ± 1.54^{d}	5.70 ± 0.58^{b}	0.795 ± 0.04^{a}

[a] Values with different letters in the same column are significantly different ($p < 0.05$).

Table 3 Film solubility, swelling, oxygen permeability (OP), water vapor permeability (WVP), and water vapor transmission rate (WVTR) of bi-layer films[a]

Sample ID	Film swelling (%)	Film solubility (%)	OP ($\times 10^{-11}$ cm^2 s^{-1} Pa^{-1})	WVP (g mm per day per m^2 per kPa)	WVTR (g per day per m^2)
C	72.15 ± 4.45^a	45.12 ± 2.25^a	2.14 ± 0.17^a	0.91 ± 0.45^a	22.61 ± 1.45^a
F1	32.15 ± 1.35^c	20.28 ± 0.95^c	1.50 ± 0.18^b	0.82 ± 0.49^c	18.70 ± 1.30^{bc}
F2	40.74 ± 2.45^b	25.45 ± 1.95^b	2.05 ± 0.17^a	0.86 ± 0.43^b	20.20 ± 1.10^b
F3	29.89 ± 1.25^c	18.50 ± 0.85^c	1.40 ± 0.25^b	0.79 ± 0.48^c	17.47 ± 1.09^c

[a] Values with different letters in the same column are significantly different ($p < 0.05$).

functionalized with MLNPs, GFE, and their combination. The control film (C), consisting of PLA_SACNFs/starch without additional fillers, exhibited the lowest contact angle of 69.6° ± 1.9, indicative of a relatively hydrophilic surface due to the abundant of polar hydroxyl groups in the starch matrix. However, the incorporation of MLNPs (F1) on the starch layer led to a notable increase in WCA to 89.5° ± 1.5, indicating enhanced surface hydrophobicity. This improvement is likely due to the presence of hydrophobic aromatic structures in lignin, which may enhance the hydrophobicity of starch films by reducing surface energy through their aromatic structure and masking hydrophilic groups. Their addition also increases surface roughness, raising the water contact angle. A similar result was observed for the enhancement of WAC for the bioplastic added with lignin nanoparticles.[57] Similarly, the inclusion of GFE, which showed a contact angle of 79.5° ± 1.5, indicates improved water resistance compared to the control but slightly lower than F1. The enhanced hydrophobicity can be attributed to strong intermolecular hydrogen bonding between the hydroxyl groups of starch and the polyphenolic compounds in GFE, which reduces the availability of free hydrophilic sites on the surface. This finding is supported by another study by ref. 58. However, the intermediate contact angle of 86.5° ± 1.5, was observed for F3 (MLNPs_GFE), which combines both MLNPs and GFE. This result suggests a synergistic effect of the two additives, where MLNPs contribute by increasing surface roughness and introducing main aromatic hydrophobic domains. A similar observation was detected for the synergic effect of Alizarin and grapefruit seed extracts in carboxymethyl cellulose/agar-based functional films.[58]

3.5 Water vapor and oxygen barrier properties

The WVTR, WVP, and OP results from Table 2 highlight the moisture and gas barrier characteristics of PLA_SACNFs/starch bilayer films incorporated with MLNPs and GFE. The control film (C) demonstrated a relatively higher WVTR (22.61 g per day per m^2) and WVP (0.91 g mm per day per m^2 per kPa) compared to the other bilayer films. However, the additional bio-additives such as MLNPs and GFE on the starch layer create a torturous path. The incorporation of MLNPs (F1) on the starch layer significantly improved barrier properties, reducing WVTR to 18.70 g per day per m^2 and WVP to 0.82 g mm per day per m^2 per kPa. The MLNPs increased the density of the film matrix by

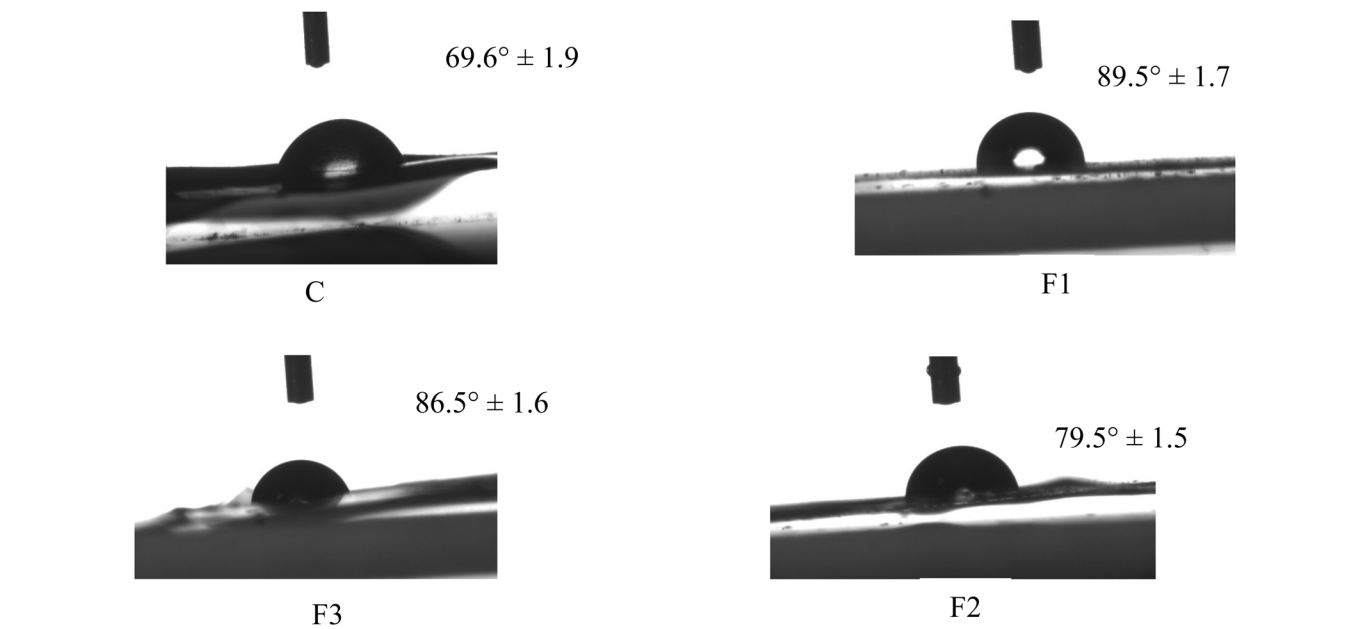

Fig. 4 Water contact angle (WCA) images of bi-layer films.

forming hydrogen bonds with starch molecules, resulting from the good compatibility between MLNPs and the starch matrix and restricting water vapor pathways. A similar result was documented where lignin nanoparticles were reinforced in the starch-based film.[59] Furthermore, the incorporation of GFE (F2) further reduced the WVTR and WVP to 20.70 g per day per m^2 and 0.86 ± 0.49 g mm per day per m^2 per kPa, respectively. The polyphenolic compounds in GFE act as cross-linking agents, enhancing the compactness of the film matrix and creating a more efficient barrier against water vapor. Similarly,[58] reported that grapefruit seed extract rich in polyphenols improves barrier properties by reinforcing the carboxymethyl cellulose/agar-based films. Moreover, the combination of MLNPs and GFE in F3 resulted in the lowest WVTR and WVP values of 17.47 g per day per m^2 and 0.79 g mm per day per m^2 per kPa, respectively. The results indicate a synergistic effect between MLNPs and GFE, balancing hydrophilicity and matrix reinforcement, creating more compact, and reducing the free volume. A similar result was documented for the addition of softwood kraft lignin nanoparticles and thymol to PBS films.[15] Morphological analysis from our research also suggests that a combination of MLNPs and GFE improves film homogeneity by reducing microvoids and minimizing molecular mobility.

Likewise, the WVTR, WVP results, and OP of the PLA_SACNFs/starch bi-layer films showed significant variations with the treatment of MLNPs and GFE. The control film (C) demonstrated the highest oxygen permeability OP at 2.14×10^{-1} cm^2 s^{-1} Pa^{-1}, which may be due to the relatively higher porous structure of the starch layer. The incorporation of MLNPs in the starch layer (F1) significantly reduced the OP to 1.50×10^{-11} cm^2 s^{-1} Pa^{-1}. This reduction is attributed to the MLNPs enhancing the tortuosity of the diffusion path within the film matrix, thereby hindering oxygen transmission. The interaction of lignin nanoparticles with the starch phase may have further improved the integrity and density of the film structure, resulting in enhanced oxygen barrier properties.[15] Similarly, the addition of GFE in the starch layer (F2) did not significantly reduce OP, as the measured value (2.05×10^{-11} cm^2 s^{-1} Pa^{-1}) remained close to that of the control. This suggests that the presence of GFE alone does not contribute significantly to oxygen barrier properties, possibly due to its hydrophilic nature and its potential to increase film porosity. A comparable trend was observed in films incorporating grapefruit seed extract into a corn starch–chitosan blend.[55] However, a slight reduction in OP values was observed in the sample containing both MLNPs and GFE (F3), which exhibited the lowest OP value of 1.40×10^{-11} cm^2 s^{-1} Pa^{-1}.

3.6 Color parameter and opacity

Table 4 demonstrates that the addition of MLNPs and GFE changed the color parameters and opacity of the PLA_SACNFs/starch bi-layer films. Fig. 5 shows the images of the MLNPs and GFE-treated bi-layer films. The neat PLA_SACNFs/starch bi-layer films were colorless and transparent. However, the bi-layer film added with MLNPs was blackish, the film added with GFE was yellowish, and the combined effect of MLNPs and GFE in the films shows pale yellow or blackish-yellow in color. The control sample (C), which had low b^* values (3.64) and slightly negative a^* (−0.50), showed the maximum brightness L^* (90.20), suggesting a light and slightly greenish-yellow color. Its opacity was the lowest of all samples (1.102 UA mm^{-1}), and its whiteness index (WI) was 90.05, indicating a clearer film, and it shows the least color difference (ΔE). However, with the addition of MLNPs (F1), the L^* value dropped to 68.60, suggesting a noticeably darker appearance compared to the control sample. As the b^* value rose to 19.17, indicating a more noticeable yellow tint, the a^* value turned positive (0.94), indicating a move towards red. As a result, the transparency was significantly diminished, as seen by the opacity rising to 1.928 UA mm^{-1} and the WI falling to 65.90. The ΔE^* value (32.03) was significantly higher than that of the control, suggesting a marked and perceptible color deviation. Similar observations have been reported in previous studies, where lignin and its derivatives impart darker shades and increased opacity to polymer films due to their natural pigmentation and light-absorbing properties.[42] On the other hand, the incorporation of GFE (F2) exhibited a moderate lightness level, with an L^* value of 76.30, indicating it was lighter than F1 and F3, yet still notably darker than the control film. The a^* value of 0.60 indicated a slight reddish tone, whereas the b^* value of 24.90 was the highest among all samples, signifying a strong yellow coloration. This pronounced yellow hue is attributable to a higher concentration of flavonoids, pigments, and phenolic compounds present in GFE. Despite the vivid yellow appearance, the film exhibited a high ΔE^* value of 29.43, indicating a notable color deviation from the reference white. The whiteness index (WI = 69.10) was marginally higher than that of F1, suggesting that although yellowness increased, overall visual whiteness was better maintained. With an opacity of 1.705 UA mm^{-1}, F2 was less transparent than the control film. These results align with earlier findings that plant-derived additives such as GFE can markedly influence film coloration and enhance light absorption, thereby improving UV-blocking properties.[55] The combination of MLNPs and GFE in F3 led to an L^* value of 69.36, accompanied by the highest a^* value (1.50), reflecting a more pronounced reddish tint. A high b^* value (22.20) also indicated significant yellowness. F3 demonstrated the greatest color difference from the control, with a ΔE^* value of 34.92, and exhibited the lowest whiteness index (WI = 63.22) along with the highest opacity (2.816 UA mm^{-1}), identifying it as the most visually dense and pigmented film among all samples. These findings align with previous studies demonstrating that melanin nanoparticles and grapefruit seed extract can significantly alter visual properties while also enhancing UV-blocking capabilities in biopolymer films.[45]

3.7 Ultraviolet and visible light transmission

The UV-Vis light transmission of the bi-layer films was studied to evaluate their potential as effective UV-shielding capacity. Fig. 6 reveals distinct trends across the four formulations: C, F1, F2, and F3. The incorporation of active compounds like MLNPs and GFE into the second layer notably altered the UV-Vis light

Table 4 Different color parameters and opacity values of bi-layer films[a]

	Color and optical properties					
Sample ID	L^*	a^*	b^*	ΔE^*	WI	Opacity (UA mm^{-1})
C	90.20 ± 1.55^{a}	-0.50 ± 0.17^{c}	3.64 ± 0.29^{c}	7.73 ± 0.51^{c}	90.05	1.102
F1	68.60 ± 2.15^{c}	0.94 ± 0.20^{ab}	15.17 ± 1.25^{b}	32.03 ± 1.75^{a}	65.90	1.928
F2	76.30 ± 0.78^{b}	0.60 ± 1.05^{b}	24.90 ± 2.86^{a}	29.43 ± 1.50^{a}	69.10	1.705
F3	69.36 ± 0.75^{c}	1.50 ± 0.80^{a}	22.20 ± 1.40^{a}	34.92 ± 1.45^{b}	63.22	2.516

[a] Values with different letters in the same column are significantly different ($p < 0.05$).

transmission of the films. All samples exhibited total UV light blockage up to 230 nm. However, the control sample without any additives in the second layer exhibited the highest UV-Vis light transmission, indicating minimal UV-shielding capability. In the range between 250 and 300 nm, incorporating MLNPs (F1) and GFE (F2) into the starch layer significantly reduced UV light transmission to a minimum (T_{300}) of 4.5% and 2.8%, respectively, as compared to the control (55.1%), whereas, the visible light transmission (T_{660}) reduces to 49.7% and 38.8% respectively as compared to control (68.9%). The enhanced UV-blocking ability of lignin-based films arises from lignin's phenolic content and conjugated aromatic structures that efficiently absorb UV radiation[60] Likewise, grapefruit flavedo extract contributes to UV protection through flavonoids such as naringin and hesperidin, which possess strong UV-absorbing conjugated systems.[2] This result aligns with previous studies that demonstrated the effectiveness of lignin derivatives and grapefruit seed extracts in improving the UV-shielding properties of polymer composites.[61,62] Interestingly, the combined effect of both fillers resulted in a substantial reduction in UV-Vis light transmission. The synergistic interaction between MLNPs and GFE enhances the shielding effect to a minimum transmission (T_{300}) of 1.3% and visible light transmission (T_{660}) of 47.4% by providing complementary absorption mechanisms. The dual functionality of these additives, MLNPs particle-based scattering and GFE's molecular UV absorption, contributes to the superior performance of F3. Similar synergistic effects have been observed in gelatin-based bi-layer films added with Pitanga leaf extracts and nisin in the second layer.[13]

3.8 TPC and TFC analysis

Table 5 shows the TPC and TFC content of PLA_SACNFs/starch bi-layer films added with MLNPs and GFE on the starch layers. Each bi-layer film displayed unique characteristics, influenced by the nature and concentration of the bio-additives used. The incorporation of bio-additives significantly enhanced the TPC and TFC of the bi-layer films. The maximum TPC (28.36 mg GAE per g) was observed in the bi-films where MLNPs and GFE were added in the starch layer (F3), as both lignin and GFE were good sources of phenolic compounds.[24,63] In contrast, the control

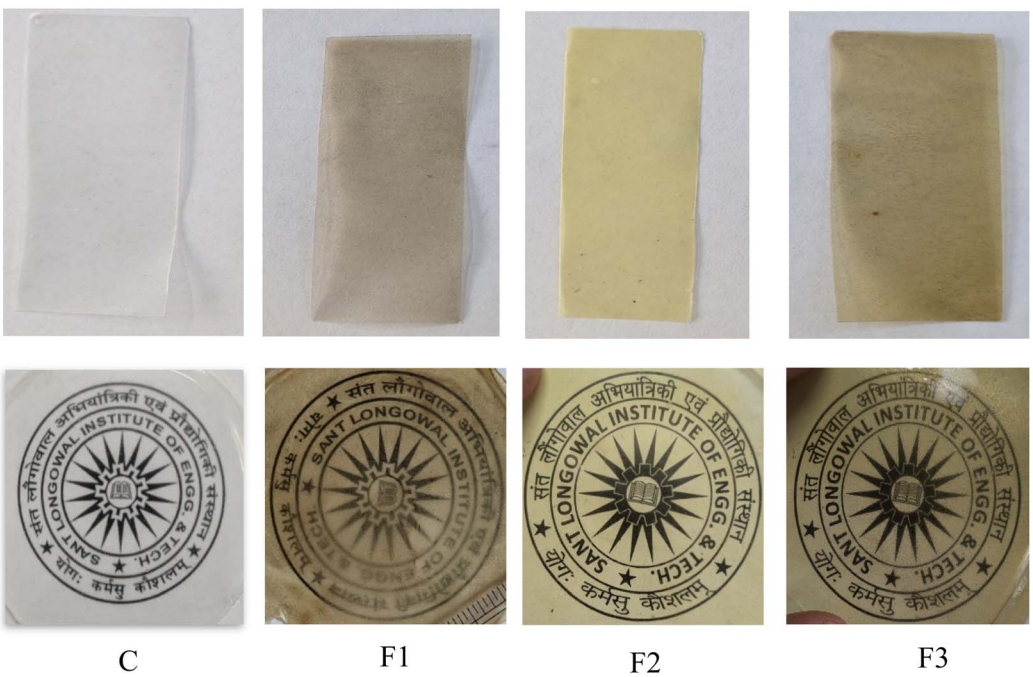

Fig. 5 Images of bi-layer films.

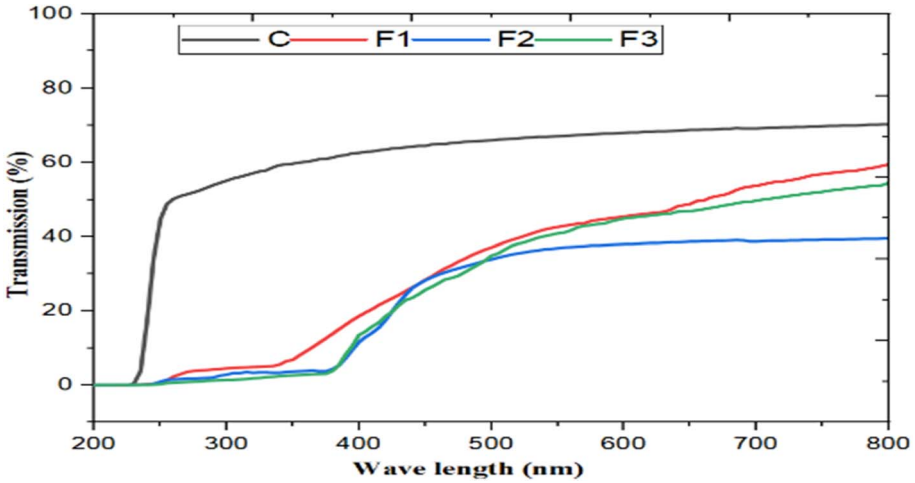

Fig. 6 UV-Vis light transmission of bi-layer films.

exhibited the lowest TPC (1.68 GAE per g) and TFC (0.045 mg QE per g), indicating minimal phenolic and flavonoid content inherent in the control sample. The addition of MLNPs (F1) resulted in a moderate increase in TPC (14.89 mg GAE per g) and TFC (2.045 mg QE per g), likely due to the presence of phenolic compounds in the lignin. However, the incorporation of GFE (F2) markedly increased the TPC (17.21 mg GAE per g) and TFC (4.409 QE/g), highlighting the high phenolic and flavonoid content of grapefruit flavedo. These findings are consistent with prior research, indicating that natural extracts from grapefruits and lignin effectively enhance bioactive compound levels in biopolymer matrices.[64,65]

3.9 Antioxidant activity (AA)

The antioxidant activity (AA) of the active bi-layer films incorporating modified lignin nanoparticles (MLNPs) and grapefruit flavedo extract (GFE) was evaluated using various free radical scavenging assays, including DPPH, ABTS, and FRAP. The addition of these bioactive components significantly enhanced the AA of the bi-layer films, as summarized in Table 5. The control sample (C) exhibited negligible antioxidant activity. The film containing only MLNPs (F1) demonstrated moderate scavenging activity, with values of 24.51% for DPPH, 4.07 μg GAE per g for ABTS, and 5.10 mg FeE per g for FRAP. In contrast, the GFE-incorporated film showed higher AA, recording 39.36% (DPPH), 6.81 μg GAE per g (ABTS), and 7.58 mg FeE per g (FRAP). Notably, the combined inclusion of both GFE and MLNPs (F3) resulted in a synergistic effect, achieving markedly enhanced antioxidant activity with values of 66.86% (DPPH), 9.64 μg GAE per g (ABTS), and 10.12 mg FeE per g (FRAP). It is a very well-known fact that lignin nanoparticles and grapefruit flavedo extract have intensified antioxidant activity.[66] This notable enhancement can be ascribed to flavonoids, such as naringin and hesperidin, along with other polyphenolic compounds in GPE.[24] On the other hand, LNPs show high antioxidant activity, which is ascribed to their phenolic hydroxyl groups, which facilitate hydrogen donation and radical scavenging.[67] Since better antioxidant activity is correlated with higher phenolic and flavonoid content, the trend is consistent with the TPC and TFC results. Antioxidant films based on different bio-polymers, including poly(vinyl alcohol), and chitosan, have recently been prepared using LNP's antioxidant potential.[3,60,66] A starch–chitosan-based antioxidant film has recently been created using GSE's potent antioxidant activity.[50] The combination of melanin nanoparticles and grapefruit seed extract in pectin/agar-based films shows maximum AA compared to individual bio-additives in the films.[45]

3.10 Anti-microbial activity

The prolongation of the food product's self-life within a packaging system is significantly influenced by its anti-microbial activity. MLNPs and GFE-incorporated PLA_SACNFs/starch bi-

Table 5 TPC, TFC, antioxidant activity, and anti-microbial activity of bi-layer films[a]

Sample ID	TPC (mg GAE per g)	TFC (mg QE per g)	DPPH (%)	ABTS (μg GAE per g)	FRAP (mg FeE per g)	Inhibition zone diameter (mm)	
						P. aeruginosa	*S. aureus*
C	1.68 ± 0.45^{c}	0.045 ± 0.01^{c}	$4.05 \pm 0.30_{c}$	0.59 ± 0.15^{c}	1.16 ± 0.10^{c}	NA	NA
F1	14.89 ± 0.55^{b}	2.045 ± 0.15^{b}	24.51 ± 0.65^{b}	4.07 ± 0.12^{b}	5.10 ± 0.16^{b}	12.50	13.40
F2	17.21 ± 0.65^{b}	4.409 ± 0.10^{b}	39.36 ± 0.45^{b}	6.81 ± 0.10^{b}	7.58 ± 0.18^{b}	13.50	15.50
F3	28.36 ± 0.95^{a}	3.918 ± 0.09^{a}	66.86 ± 2.50^{a}	9.64 ± 0.30^{a}	10.12 ± 0.90^{a}	16.50	22.50

[a] Values with different letters in the same column are significantly different ($p < 0.05$).

layer films were tested for their anti-microbial effectiveness against Gram-positive (*S. aureus*) and Gram-negative (*P. aeruginosa*) bacteria by measuring the zone of inhibition in diameter (Table 5 and Fig. S1). The fact that there was no discernible antimicrobial activity in the control sample (C) suggests that the base polymer matrix by itself lacks inherent anti-microbial qualities. However, the addition of GFE and MLNPs greatly improved the film's antibacterial activity. Among the modified films, F1 (MLNPs) displayed moderate antimicrobial activity, with inhibition zone diameters of 12.50 mm for *P. aeruginosa* and 13.40 mm for *S. aureus*. This enhancement is likely attributed to the inclusion of lignin nanoparticles (LNPs), which are known to possess antimicrobial properties by disrupting microbial cell membranes and inducing the generation of reactive oxygen species (ROS).[60] The F2 (GFE) sample exhibited even greater antimicrobial efficacy, displaying inhibition zones of 13.50 mm and 15.50 mm against *P. aeruginosa* and *S. aureus*, respectively. This increased activity can be credited to the polyphenolic compounds present in grapefruit flavedo extract (GFE), such as naringin and hesperidin, which are recognized for their antimicrobial potential primarily through interactions with bacterial cell walls that compromise membrane integrity and ultimately lead to cell death.[68] The most pronounced antimicrobial performance was observed in F3 (MLNPs_GFE), which showed inhibition zones of 16.50 mm and 22.50 mm for *P. aeruginosa* and *S. aureus*, respectively. This superior effect is likely due to the synergistic combination of modified lignin nanoparticles (MLNPs) and GFE, offering a multifaceted antimicrobial mechanism involving metal ion release, ROS generation, and polyphenol-mediated disruption of microbial cells. These findings align with previous studies that have demonstrated the synergistic effect of grapefruit seed extract and curcumin on the poly(vinyl alcohol)-based films, enhanced antimicrobial efficacy.[69] The synergistic effects observed in F3 highlight the potential of these bi-layer films for applications in active food packaging and biomedical fields where antimicrobial properties are essential.

3.11 DSC analysis

DSC was conducted to assess the thermal behavior of PLA_SACNFs/starch bi-layer films added with MLNPs and GFE, as depicted in Fig. 7a. Table 6 presents DSC parameters (T_g, T_m, and ΔH_m) of the bi-layer films. The obtained thermal transitions (T_g, T_c, and T_m) are critical for determining the processing window and service temperature range of the packaging materials. The glass transition temperature (T_g) defines the lower operational limit where polymer chains gain mobility. The T_g increased from 55.32 °C (control) to 56.81 °C (F1) and 60.47 °C (F2), indicating stronger interfacial interactions and restricted chain mobility. The rise in T_g value for F2 indicates that GFE, maybe *via* hydrogen bonding, improves molecular interactions inside the polymer matrix.[70] The combined action of MLNPs and GFE, which may disrupt the polymer network, is suggested by the reduced T_g value for F3. This enhancement reflects improved dimensional stability and rigidity, which are desirable for packaging exposed to moderate heat. The melting transitions (T_{m_1} and T_{m_2}) determine the upper processing and sealing range. In the control film, T_{m_1} (123.57 °C) and T_{m_2} (148.16 °C) represent less ordered and more ordered crystalline regions, respectively. With MLNP addition (F1), T_{m_2} increased to 150.15 °C and ΔH_{m_2} rose markedly to 18.94 J g^{-1}, demonstrating improved crystalline structure organization and enhanced heat resistance.[3] Conversely, GFE incorporation (F2) lowered T_{m_1} to 108.97 °C and reduced ΔH_{m_2}, indicating that polyphenols partially disrupted crystallinity, resulting in greater flexibility but lower thermal endurance.[71] The hybrid film (F3) showed intermediate T_m values (T_{m_1} = 121.78 °C; T_{m_2} = 151.80 °C) and moderate ΔH_m (10.48 and 3.16 J g^{-1}), reflecting a balanced effect of reinforcement and plasticization. A distinct crystallization temperature (T_c = 118.47 °C) was observed only in F1, confirming that MLNPs act as nucleating agents, facilitating chain alignment and faster solidification during processing. The elevated T_c further supports improved thermal formability. Overall, MLNP addition (F1) enhanced chain ordering, crystallinity, and heat resistance, broadening the usable temperature range and making it more suitable for heat-sealable, thermally stable active packaging. Different researchers have found similar results where lignin nanoparticles enhance the thermal stability of composite films.[3,15] In contrast, GFE (F2) imparted flexibility and lower processing temperature suitability, while the combined film (F3) achieved an optimal balance between rigidity and ductility.

3.12 TGA analysis

The thermal behavior of the PLA_SACNFs/starch bi-layer films added with MLNPs and GFE (C, F1, F2, and F3) were evaluated through TGA analysis. Fig. 7b and c shows the TGA and DTG diagram of the bi-layer films. The different thermal parameters that include T_{onset}, T_{max}, and $W_{residue}$ at 500 °C are summarized in Table 6. Mainly, the reduction of weight loss occurs in four distinct phases. In the initial phase, temperature between 35 °C and 175 °C was likely due to the dehydration of water vapor from the bi-layer films. Moreover, in the second phase, from 175 °C to 250 °C, weight loss was minimal, indicating the maximum thermal stability. The third phase, between 250 °C and 374 °C, found an accelerated thermal breakdown of the bi-layer films at elevated temperatures. Finally, the fourth phase, above 400 °C, degradation involves the oxidation and breakdown of short carbon chains, producing volatile low-molecular-weight products and residual carbon.[46]

The T_{onset} values show that the inclusion of MLNPs and GFE enhanced the film's degradation temperature. As shown in Table 6, the control sample (C) showed the lowest T_{onset} at 267.30 °C, indicating a lower level of thermal resistance. The incorporation of MLNPs in the F1 film significantly enhanced its thermal stability, as indicated by a notable increase in T_{onset} to 284.50 °C. Similarly, the T_{max} value followed the same trend, with F1 exhibiting the highest T_{max} at 327.30 °C, compared to the control film's maximum degradation at 319.50 °C. These results suggest that MLNPs act as effective reinforcing fillers, improving the film's heat resistance. Comparable improvements in thermal properties have been reported with the

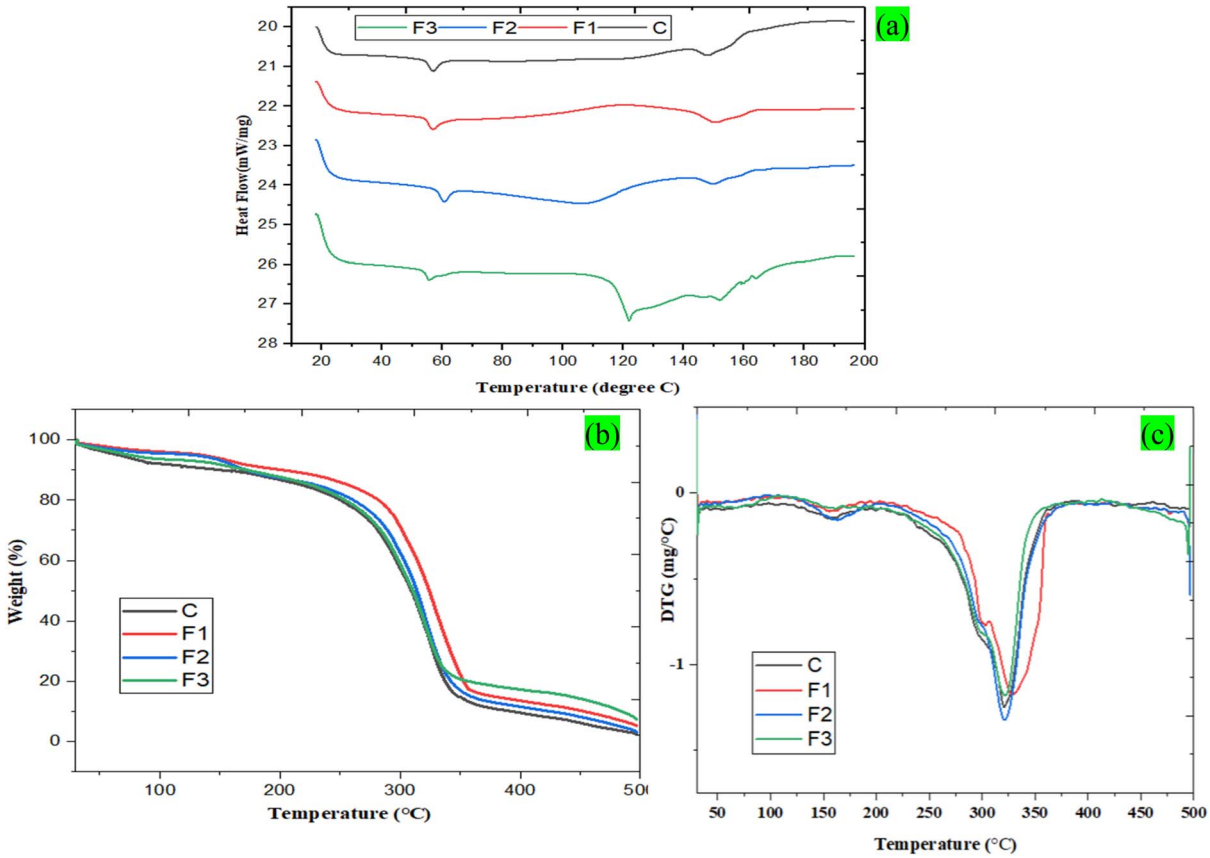

Fig. 7 DSC (a) and TGA (b and c) thermograms of bi-layer films.

addition of lignin nanoparticles to starch- and chitosan-based films.[42,66] The film containing GFE (F2) showed a moderate enhancement in thermal stability, achieving a T_{onset} of 273.30 °C and a T_{max} of 321.40 °C. Although GFE contributed to thermal improvement, its impact was less pronounced than that of MLNPs. This aligns with earlier studies demonstrating that citrus flavedo extracts, such as orange peel, provide antioxidant-based thermal protection in PP and PLA films, though their effect is often secondary to that of inorganic fillers.[71] Interestingly, the F3 film recorded a T_{max} of 322.50 °C and a T_{onset} of 268.50 °C. While its T_{onset} was lower than those of F1 and F2, its T_{max} was comparable to that of F1, indicating a complex interaction between the additives used. This shows that while MLNPs and GFE have stabilizing effects on their own, their interaction may complicate degradation kinetics, maybe because of different interfacial adhesion or differences in their mechanisms of thermal protection. However, the addition of MLNPs and GFE increases the final char residue (6.90%) of the films. The development of thermally stable char structures is probably the cause of the higher residue content in films containing MLNPs and GFE, which indicates better carbonization and thermal stability. Similar to the findings of the present study, a slight increase in char residue and thermal stability was observed upon the incorporation of lignin nanoparticles and grapefruit seed extract into biopolymers.[3,45] Additionally, all films containing MLNPs and/or GFE exhibited higher residual char (up to 6.90%), reflecting enhanced carbonization and improved thermal stability. These results suggest that F1 films, in particular, possess a broader thermal processing window and can maintain structural integrity at higher temperatures, making them suitable for packaging applications requiring moderate heat resistance. The TGA findings provide practical

Table 6 DSC parameters and TGA parameters of bi-layer films[a]

Sample ID	T_g (°C)	T_c	T_{m_1}	T_{m_2}	ΔH_{m_1} (J g^{-1})	ΔH_{m_2} (J g^{-1})	T_{onset} (°C)	T_{max} (°C)	$W_{residue}$ (%) at 500 °C
C	56.65	—	123.57	148.16	—	2.475	267.30	320.50	2.43
F1	56.81	118.47	—	150.15	—	18.94	284.50	327.30	5.27
F2	60.41	—	108.97	149.98	13.314	6.49	273.30	321.22	3.15
F3	55.57	—	121.78	151.80	10.48	3.164	268.50	321.50	6.90

[a] T_g: glass transition temperature, T_m: melting temperature, T_c: crystallization temperature, ΔH_{m_i}: melting enthalpy values, T_{onset}: onset degradation temperature, T_{max}: maximum degradation temperature, $W_{residue}$ (%) residual weight at 500 °C.

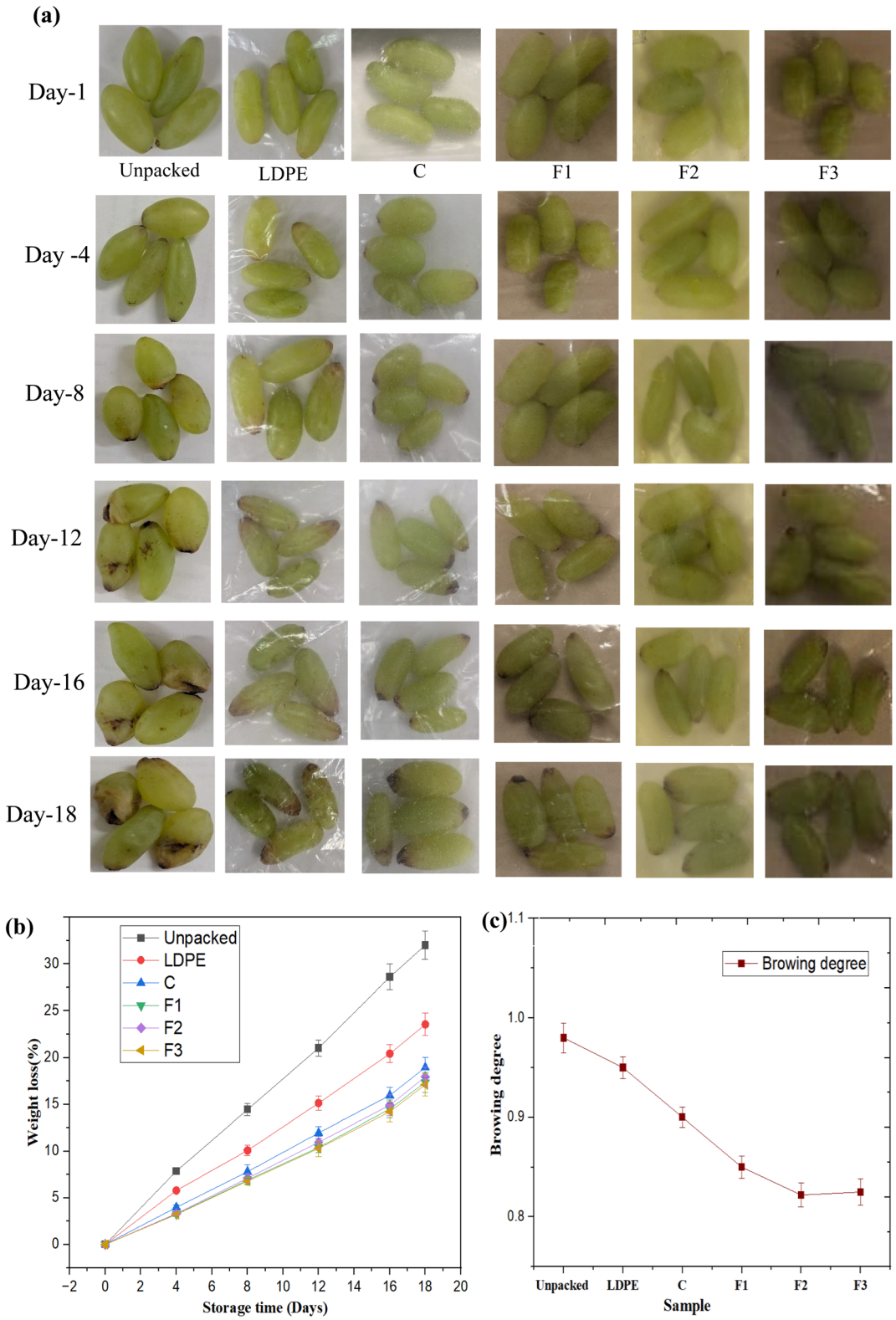

Fig. 8 (a) Visual assessment of freshness and shelf life, (b) weight loss (%), and (c) browning inhibition of unpackaged grapes and packed with LDPE, C, F1, F2 and F3 active films.

insights into the film's performance, materials with higher T_{onset} and T_{max} are less likely to deform or degrade during processing, storage, or thermal exposure, thereby extending their functional applicability in packaging.

3.13 Functional efficiency of active films

3.13.1 Visual attributes. Fig. 8a illustrates the visual appearance of unpackaged grapes and those packed in LDPE

and active bi-layer films (C, F1, F2, F3) over the period of 18 days. At day 1, all samples showed a fresh and uniform bright green color, reflecting initial quality consistency. By day 4, unpackaged grapes and those stored in LDPE films began to exhibit slight browning and shriveling, which progressed rapidly and became severe by day 8, and 12, leading to significant discoloration and loss of quality by day 16 and 18. These changes can be attributed to moisture loss, dehydration, and oxidative reactions of polyphenols.[72]

In contrast, grapes stored in active bi-layer films demonstrated improved visual preservation, with the extent of effectiveness depending on the film composition. Grapes stored in active bi-layer films retained their quality for longer times. Grapes stored in the control bi-layer film (C) showed shrinkage and browning after day 12, while those in F1 film showed delayed deterioration but still show some shrinkages by day 16 and prominent at day 18. However, grapes packed in F2 (GFE) and F3 (MLNPs + GFE) films both showed only slight discoloration by day 18, indicating almost similar effectiveness in preserving visual quality. This can be attributed to the strong antioxidant activity of GFE and the high UV-blocking capacity of both films, which together suppressed oxidative browning and minimized light-induced degradation. These outcomes are consistent with earlier studies, which demonstrated that fruit discoloration is primarily governed by oxidative processes, and that incorporating strong natural antioxidants into active films is highly effective in slowing visible quality loss. Similar preservation effects have also been reported for grapes, where chitosan–lignosulfonate coatings reduced decay and helped retain color and firmness during storage,[73] and alginate films enriched with grapefruit seed extract minimized browning and maintained the natural visual appearance of table grapes.[74] Overall, F2 and F3 packaging performed equally well in preserving the visual quality of grapes during storage.

3.13.2 Weight loss. Weight loss increased progressively across all treatments during the 18-day storage period due to moisture evaporation and respiration, which, when excessive, can cause shriveling and reduce consumer acceptability[75]. As illustrated in Fig. 8b, weight loss rose steadily over time for all packaging conditions. Unpacked grapes exhibited the highest loss, exceeding 30% by day 18, indicating rapid dehydration in the absence of a protective barrier. Grapes packaged in LDPE films showed comparatively lower weight loss than unpacked samples; however, the reduction was modest, reflecting the limited moisture retention capability of LDPE films. Grapes packed with active films (C, F1, F2, F3) exhibited significantly lower weight loss compared to unpacked samples throughout storage. Among these, F3 consistently demonstrated the least weight loss, followed by F1 and F2, while sample C showed slightly higher values than the formulated active films. The superior performance of F3 can be attributed to its enhanced barrier properties, resulting from the synergistic effect of bioactive components (MLNPs and GFE) and a higher concentration of active compounds. These properties improve water vapor transmission rate (WVTR), oxygen permeability (OP), UV barrier capacity, and antioxidant activity, which collectively help create a modified internal atmosphere and slow down respiration. Additionally, the antioxidant functionality of F3 may have contributed to reduced metabolic activity. Consequently, F3 packaging effectively limited moisture loss and maintained grape quality during storage, highlighting its potential as an advanced active packaging solution for extending shelf life. Similar synergistic effects have been reported in active packaging studies, where combining two bioactive compounds (*e.g.*, essential oils with nanoparticles or polyphenols) significantly reduced weight loss and extended shelf life compared to single-active films[76–78].

3.13.3 Antibrowning analysis. Colour is an essential sensory attribute that determines the visual appeal and overall quality of grapes. However, browning naturally occurs during storage due to enzymatic oxidation and microbial activity, which leads to nutrient degradation, reduced shelf life, and decreased market value. Therefore, browning is strongly associated with the antioxidant and antimicrobial potential of the packaging material.[79] Fig. 8c presents the browning degree of unpacked grapes and those packed with different active films. The results showed that unpacked grapes exhibited the highest browning, likely due to the oxidation of polyphenols and lipids in the absence of protective packaging. Among the active films, F3 demonstrated the lowest browning degree, followed by F2 and F1, whereas LDPE and the control film (C) were less effective. The superior performance of the F3 film can be attributed to multiple factors. Firstly, the antibacterial effect of GFE reduces microbial growth on the grape surface. Secondly, the antioxidant properties of MLNPs protect polyphenolic compounds from oxidation. Furthermore, the UV-blocking capability of the film minimizes light-induced oxidative reactions, which collectively delay enzymatic browning and help maintain the visual quality of grapes during storage. These findings align with previous studies reporting that dual-functional films with antioxidant and antimicrobial activity effectively delay enzymatic browning in fruits.[79,80].

4 Conclusion

This study successfully developed and characterized PLA_SACNFs/starch bi-layer film reinforced with rice straw CNFs and functionalised with organosolv MLNPs and/or GFE. The findings pointed out that incorporating MLNPs and GFE significantly enhanced the film's physicochemical, barrier, thermal, and bio-functional properties. The solubility, swelling index, and moisture content of the films significantly reduce with the addition of MLNPs and GFE. The incorporation of individual fillers (MLNPs, GFE) also enhances the WCA of films. Furthermore, UV-Vis analysis revealed the film's enhanced UV-protection properties. The combined effect of MLNPs and GFE on the bi-layer films shows the maximum barrier properties (WVTR, WVP, and OTR). Mechanical analysis reveals that MLNPs improved tensile strength by 25.30%, while GFE contributed to flexibility. However, the combined effect does not show any significant change in the strength properties. Structural analysis through XRD and FT-IR verified the interaction of MLNPs and GFE within the polymer matrix, contributing to improved film integrity. TGA and DSC analysis also reveal that individual fillers (MLNPs, GFE) enhance the thermal

properties. However, FE-SEM analysis also confirmed the uniform distribution of MLNPs, and no crack was observed in GFE dispersed in the starch matrix. The synergic effect of MLNPs and GFE significantly enhanced the film's bio-functional properties. Antioxidant tests confirmed a notable increase in radical scavenging activity, and antibacterial analysis demonstrated strong inhibition against *P. aeruginosa* and *S. aureus,* highlighting the potential of these films for active packaging applications. Importantly, active packaging trials confirmed that the film added with MLNPs and GFE shows least weight loss and browning of green grapes, extending their shelf life up to 18 days under refrigeration condition. These findings demonstrate that the developed bi-layer films represent a sustainable alternative to conventional plastics, aligning with circular economy principles while simultaneously reducing plastic waste and postharvest food losses, thereby contributing to food security and sustainable packaging systems.

Consent for publication

All authors agree that this research report may be published.

Author's contributions

Makdud Islam: writing – original manuscript, editing, conceptualization, methodology, data curation, formal analysis; A. S. K. Sinha: review & editing, visualization, project administration, Kamlesh Prasad: review & editing, visualization, project administration.

Conflicts of interest

This work doesn't have any conflict of interest.

Data availability

All the data generated or analysed during this study are included in the manuscript.

Supplementary information (SI) is available. See DOI: **https://doi.org/10.1039/d5fb00561b**.

Acknowledgements

All the authors express their gratitude to the Director, Sant Longowal Institute of Engineering and Technology (SLIET), Longowal, Punjab and special thanks to Mr Ramnik Agrawal, Senior Technician, for assisting in conducting the experiments.

References

1 S. Fakhreddin, F. Kaveh and M. Schmid, Facile Fabrication of Transparent High-Barrier Poly (Lactic Acid) -Based Bilayer Films with Antioxidant/Antimicrobial Performances, *Food Chem.*, 2022, **384**, 132540, DOI: **10.1016/j.foodchem.2022.132540**.

2 L. F. Wang and J. W. Rhim, Grapefruit Seed Extract Incorporated Antimicrobial LDPE and PLA Films: Effect of Type of Polymer Matrix, *LWT*, 2016, **74**, 338–345, DOI: **10.1016/j.lwt.2016.07.066**.

3 W. Yang, J. S. Owczarek, E. Fortunati, M. Kozanecki, A. Mazzaglia, G. M. Balestra, J. M. Kenny, L. Torre and D. Puglia, Antioxidant and Antibacterial Lignin Nanoparticles in Polyvinyl Alcohol/Chitosan Films for Active Packaging, *Ind. Crops Prod.*, 2016, **94**, 800–811, DOI: **10.1016/j.indcrop.2016.09.061**.

4 L. Shao, Y. Xi and Y. Weng, Recent Advances in PLA-Based Antibacterial Food Packaging and Its Applications, *Molecules*, 2022, **27**(18), DOI: **10.3390/molecules27185953**.

5 B. K. Dejene and A. D. Gudayu, Achieving Performance and Functionality in PLA-Based Packaging: Insights from Hybrid Composites with False Banana (Enset) Fiber and ZnO Nanoparticles, *J. Thermoplast. Compos. Mater.*, 2024, **0**(0), 1–31, DOI: **10.1177/08927057241288125**.

6 O. O. Oluwasina and I. O. Awonyemi, Citrus Peel Extract Starch - Based Bioplastic : Effect of Extract Concentration on Packed Fish and Bioplastic Properties, *J. Polym. Environ.*, 2021, **29**(6), 1706–1716, DOI: **10.1007/s10924-020-01990-7**.

7 L. C. Leites, P. Julia, M. Frick and T. I. Cristina, Influence of the Incorporation Form of Waste from the Production of Orange Juice in the Properties of Cassava Starch-Based Films, *Food Hydrocolloids*, 2021, **117**, 1–11.

8 T. Anukiruthika, P. Sethupathy, A. Wilson, K. Kashampur, J. A. Moses and C. Anandharamakrishnan, Multilayer Packaging: Advances in Preparation Techniques and Emerging Food Applications, *Compr. Rev. Food Sci. Food Saf.*, 2020, **19**(3), 1156–1186, DOI: **10.1111/1541-4337.12556**.

9 C. Martins, F. Vilarinho, A. Sanches, M. Andrade, A. V. Machado, M. C. Castilho, A. Sá, A. Cunha, M. F. Vaz and F. Ramos, Active Polylactic Acid Film Incorporated with Green Tea Extract : Development , Characterization and e Ff Ectiveness, *Ind. Crops Prod.*, 2018, **123**, 100–110, DOI: **10.1016/j.indcrop.2018.06.056**.

10 N. Gürler, S. Pasa and H. Temel, Silane Doped Biodegradable Starch-PLA Bilayer Films for Food Packaging Applications: Mechanical, Thermal, Barrier and Biodegradability Properties, *J. Taiwan Inst. Chem. Eng.*, 2021, **123**, 267–271, DOI: **10.1016/j.jtice.2021.05.030**.

11 Y. Wang, K. Wang, M. Chen, P. Zhao, Y. Wang, X. Wang, X. Han and J. Wang, Development and Characterization of Biodegradable Bilayer Packaging Films Based on Corn Starch-Polylactic Acid as Raw Material, *J. Food Meas. Charact.*, 2024, **18**(1), 625–639, DOI: **10.1007/s11694-023-02198-8**.

12 C. Aravindhan and T. T. Thiyaku, Characterization of PLA/PCL Biocomposite Food Packaging Film Using Orange Peel Essential Oil Bio-Plasticizer and Lignin Biocompatibilizer, *Polym. Bull.*, 2024, **82**(1), 21–39, DOI: **10.1007/s00289-024-05526-0**.

13 C. G. Luciano, M. M. Rodrigues, R. V. Lourenço, A. M. Q. B. Bittante, A. M. Fernandes and P. José, Bi-Layer Gelatin Film : Activating Film by Incorporation of " Pitanga " Leaf Hydroethanolic Extract and/or Nisin in the Second Layer, *Food Bioprocess Technol.*, 2021, 106–119.

14 E. F. Sucinda, M. S. A. Majid, M. J. M. Ridzuan, E. M. Cheng, H. A. Alshahrani and N. Mamat, Development and Characterisation of Packaging Film from Napier Cellulose Nanowhisker Reinforced Polylactic Acid (PLA) Bionanocomposites, *Int. J. Biol. Macromol.*, 2021, **187**, 43–53.

15 A. J. Basbasan, B. Hararak, C. Winotapun, W. Wanmolee, W. Chinsirikul, P. Leelaphiwat, V. Chonhenchob and K. Boonruang, Lignin Nanoparticles for Enhancing Physicochemical and Antimicrobial Properties of Polybutylene Succinate/Thymol Composite Film for Active Packaging, *Polymers*, 2023, **15**(4), 989, DOI: **10.3390/polym15040989**.

16 S. Roy, W. Zhang, D. Biswas, R. Ramakrishnan and J. W. Rhim, Grapefruit Seed Extract-Added Functional Films and Coating for Active Packaging Applications: A Review, *Molecules*, 2023, **28**(2), 1–17, DOI: **10.3390/molecules28020730**.

17 S. Roy and J. W. Rhim, Fabrication of Pectin/Agar Blended Functional Film: Effect of Reinforcement of Melanin Nanoparticles and Grapefruit Seed Extract, *Food Hydrocolloids*, 2021, **118**, 106823, DOI: **10.1016/j.foodhyd.2021.106823**.

18 J. P. Pinto, M. H. Anandalli, A. A. Hunashyal, Priyadarshini, S. P. Masti, R. B. Chougale, V. Gudihal and R. F. Bhajantri, Carbon Nanotubes Reinforced Chitosan/Poly (1-Vinylpyrrolidone-Co-Vinyl Acetate) Films: A Sustainable Approach for Optoelectronic Applications, *J. Mater. Sci.: Mater. Electron.*, 2025, **36**(17), 1–12, DOI: **10.1007/s10854-025-15058-6**.

19 M. N. Gunaki, S. P. Masti, L. K. Kurabetta, S. Madihalli, A. A. Hunashyal, R. B. Chougale, V. Holeyannavar and S. Kumar Vootla, Chitosan-Encapsulated CuO Nanoparticles Reinforced Multifunctional Chitosan/Gelatine Nanocomposite Films: A Promising Extension of Cherry and Grape Shelf Life, *J. Environ. Chem. Eng.*, 2025, **13**(5), 118397, DOI: **10.1016/j.jece.2025.118397**.

20 A. A. Hunashyal, S. P. Masti, L. K. Kurabetta, M. N. Gunaki, S. Madihalli, J. P. Pinto, M. Megalamani, B. Thokchom, R. B. Yarajarla and R. B. Chougale, Neem Leaf-Derived Carbon Dot-Embedded Chitosan-Based Active Films: A Sustainable Approach to Prolong the Shelf Life of Prawns, *Sustainable Food Technol.*, 2025, **2**, 382–391, DOI: **10.1039/d5fb00358j**.

21 M. Islam, A. S. K. Sinha and K. Prasad, Organosolv Delignification of Rice Straw Cellulose Fiber for Functional Food Packaging, *Cellulose*, 2024, **31**, 9191–9214, DOI: **10.1007/s10570-024-06125-y**.

22 W. Yang, E. Fortunati, D. Gao, G. M. Balestra, G. Giovanale, X. He, L. Torre, J. M. Kenny and D. Puglia, Valorization of Acid Isolated High Yield Lignin Nanoparticles as Innovative Antioxidant/Antimicrobial Organic Materials, *ACS Sustain. Chem. Eng.*, 2018, **6**(3), 3502–3514, DOI: **10.1021/acssuschemeng.7b03782**.

23 X. He, F. Luzi, W. Yang, Z. Xiao, L. Torre, Y. Xie and D. Puglia, Citric Acid as Green Modifier for Tuned Hydrophilicity of Surface Modified Cellulose and Lignin Nanoparticles, *Sustainable Chem. Eng.*, 2018, **6**(8), 9966–9978, DOI: **10.1021/acssuschemeng.8b01202**.

24 M. Islam, S. Malakar, U. Dwivedi, P. K. Prabakar, A. Kishore and A. Kumar, Impact of Different Drying Techniques on Grapefruit Peels and Subsequent Optimization of Ultrasonic Extraction Conditions for Bioactive Compounds, *J. Food Process Eng.*, 2022, 1–16, DOI: **10.1111/jfpe.14331**.

25 A. Abdulkhani, J. Hosseinzadeh, A. Ashori, S. Dadashi and Z. Takzare, Preparation and Characterization of Modified Cellulose Nanofibers Reinforced Polylactic Acid Nanocomposite, *Polym. Test.*, 2014, **35**, 73–79, DOI: **10.1016/j.polymertesting.2014.03.002**.

26 H. Rostamzad, S. Yousef, B. Shabanpour, S. M. Ojagh and S. M. Mousavi, Improvement of Fish Protein Film with Nanoclay and Transglutaminase for Food Packaging, *Food Packag. Shelf Life*, 2016, **7**, 1–7, DOI: **10.1016/j.fpsl.2015.10.001**.

27 M. Hassannia-Kolaee, F. Khodaiyan, R. Pourahmad and I. Shahabi-Ghahfarrokhi, Development of Ecofriendly Bionanocomposite: Whey Protein Isolate/Pullulan Films with Nano-SiO2, *Int. J. Biol. Macromol.*, 2016, **86**, 139–144, DOI: **10.1016/j.ijbiomac.2016.01.032**.

28 ASTM, *Standard Test Method for Tensile Properties of Thin Plastic Sheeting*, ASTM International, West Conshohocken, PA, 2010.

29 A. O. A. C., *Official Methods of Analysis*, Association of Official Analytical Chemists, Washington, DC, 18th edn, 2005.

30 N. Nordin, S. H. Othman, S. A. Rashid and R. K. Basha, Effects of Glycerol and Thymol on Physical, Mechanical, and Thermal Properties of Corn Starch Films, *Food Hydrocolloids*, 2020, **106**, 105884, DOI: **10.1016/j.foodhyd.2020.105884**.

31 X. He, F. Luzi, X. Hao, W. Yang, Z. Xiao, Y. Xie and D. Puglia, Thermal, Antioxidant and Swelling Behaviour of Transparent Polyvinyl (Alcohol) Films in Presence of Hydrophobic Citric Acid-Modified Lignin Nanoparticles Xiaoyan, *Int. J. Biol. Macromol.*, 2019, **127**, 665–676, DOI: **10.1016/j.ijbiomac.2019.01.202**.

32 C. M. Machado, P. Benelli and I. C. Tessaro, Study of Interactions between Cassava Starch and Peanut Skin on Biodegradable Foams, *Int. J. Biol. Macromol.*, 2020, **147**, 1343–1353, DOI: **10.1016/j.ijbiomac.2019.10.098**.

33 ASTM E96-00, *Standard Test Methods for Gravimetric Determination of Water Vapor Transmission Rate of Materials*, ASTM International, West Conshohocken, PA, 2000, DOI: **10.1520/E0096**.

34 ASTM, *Standard Test Method for Oxygen Gas Transmission Rate through Plastic Film and Sheeting Using a Coulometric Sensor, Method D 3985-05*, American Society for Testing and Materials, Philadelphia, 2004.

35 C. M. Bitencourt, P. J. A. Sobral and R. A. Carvalho, Food Hydrocolloids Gelatin-Based Fi Lms Additivated with Curcuma Ethanol Extract : Antioxidant Activity and Physical Properties of Fi Lms, *Food Hydrocolloids*, 2014, **40**, 145–152, DOI: **10.1016/j.foodhyd.2014.02.014**.

36 D. Das, P. S. Panesar and C. S. Saini, Effect of Montmorillonite (MMT) on the Properties of Soybean Meal

Protein Isolate-Based Nanocomposite Film Loaded with Debittered Kinnow Peel Powder, *Food Res. Int.*, 2024, **185**, 114292, DOI: 10.1016/j.foodres.2024.114292.

37 H. H. S. Abdel-Naeem, K. I. Sallam and N. M. L. Malak, Improvement of the Microbial Quality, Antioxidant Activity, Phenolic and Flavonoid Contents, and Shelf Life of Smoked Herring (Clupea Harengus) during Frozen Storage by Using Chitosan Edible Coating, *Food Control*, 2021, **130**, 108317.

38 H. Lian, Y. Peng, J. Shi and Q. Wang, Effect of Emulsifier Hydrophilic-Lipophilic Balance (HLB) on the Release of Thyme Essential Oil from Chitosan Films, *Food Hydrocolloids*, 2019, **97**(61), 105213, DOI: 10.1016/j.foodhyd.2019.105213.

39 S. M. Eskandarabadi, M. Mahmoudian, K. R. Farah, A. Abdali, E. Nozad and M. Enayati, Active Intelligent Packaging Film Based on Ethylene Vinyl Acetate Nanocomposite Containing Extracted Anthocyanin, Rosemary Extract and ZnO/Fe-MMT Nanoparticles, *Food Packag. Shelf Life*, 2019, **22**, 100389, DOI: 10.1016/j.fpsl.2019.100389.

40 M. Alboofetileh, M. Rezaei, H. Hosseini and M. Abdollahi, Antimicrobial Activity of Alginate/Clay Nanocomposite Films Enriched with Essential Oils against Three Common Foodborne Pathogens, *Food Control*, 2014, **36**(1), 1–7, DOI: 10.1016/j.foodcont.2013.07.037.

41 C. Wang, X. Zhang, Y. Gao, Y. Han and X. Wu, Path Analysis of Non-Enzymatic Browning in Dongbei Suancai during Storage Caused by Different Fermentation Conditions, *Food Chem.*, 2021, **335**, 127620.

42 X. Sun, Q. Li, H. Wu, Z. Zhou, S. Feng, P. Deng, H. Zou, D. Tian and C. Lu, Sustainable Starch/Lignin Nanoparticle Composites Biofilms for Food Packaging Applications, *Polymers*, 2023, **15**(8), 1959, DOI: 10.3390/polym15081959.

43 M. Meenu, A. K. Pujari, S. Kirar, A. Thakur, M. Garg and J. Bhaumik, Development of Bionanocomposite Packaging Films Based on Lignin Nanoencapsulated Anthocyanins Extracted from Agro-Waste for Enhancing the Post-Harvest Shelf Life of Tomatoes, *Sustainable Food Technol.*, 2025, **3**(2), 414–424, DOI: 10.1039/d4fb00342j.

44 M. Kaya, S. Khadem, Y. S. Cakmak, M. Mujtaba, S. Ilk, L. Akyuz, A. M. Salaberria, J. Labidi, A. H. Abdulqadir and E. Deligöz, Antioxidative and Antimicrobial Edible Chitosan Films Blended with Stem, Leaf and Seed Extracts of Pistacia Terebinthus for Active Food Packaging, *RSC Adv.*, 2018, **8**(8), 3941–3950, DOI: 10.1039/c7ra12070b.

45 S. Roy and J. W. Rhim, Fabrication of Pectin/Agar Blended Functional Film: Effect of Reinforcement of Melanin Nanoparticles and Grapefruit Seed Extract, *Food Hydrocolloids*, 2021, **118**, 106823, DOI: 10.1016/j.foodhyd.2021.106823.

46 J. Muller, C. González and A. Chiralt, Poly (Lactic) Acid (PLA) and Starch Bilayer Films, Containing Cinnamaldehyde,Obtained by Compression Moulding, *Eur. Polym. J.*, 2017, **95**, 56–70, DOI: 10.1016/j.eurpolymj.2017.07.019.

47 H. Trevisan and C. A. Rezende, Pure, Stable and Highly Antioxidant Lignin Nanoparticles from Elephant Grass, *Ind. Crops Prod.*, 2020, **145**, 112105, DOI: 10.1016/j.indcrop.2020.112105.

48 Z. Yuan, X. Shang, J. Fang and H. A. Li, Simple Method for Preparation of Lignin/TiO2 Nanocomposites by Sulfonation Degree Regulation and Their Application in Polyurethane Films, *Int. J. Biol. Macromol.*, 2022, **198**, 18–25, DOI: 10.1016/j.ijbiomac.2021.12.108.

49 C. Shi, J. Cui, X. Yin, Y. Luo and Z. Zhou, Grape Seed and Clove Bud Extracts as Natural Antioxidants in Silver Carp (Hypophthalmichthys Molitrix) Fillets during Chilled Storage: Effect on Lipid and Protein Oxidation, *Food Control*, 2014, **40**(1), 134–139, DOI: 10.1016/j.foodcont.2013.12.001.

50 P. Jha, Effect of Grapefruit Seed Extract Ratios on Functional Properties of Corn Starch-Chitosan Bionanocomposite Films for Active Packaging, *Int. J. Biol. Macromol.*, 2020, **163**, 1546–1556, DOI: 10.1016/j.ijbiomac.2020.07.251.

51 R. Vijayakumar, Y. Sivaraman, K. M. Pavagada Siddappa and J. P. R. Dandu, Synthesis of Lignin Nanoparticles Employing Acid Precipitation Method and Its Application to Enhance the Mechanical, UV-Barrier and Antioxidant Properties of Chitosan Films, *Int. J. Polym. Anal. Charact.*, 2022, **27**(2), 99–110, DOI: 10.1080/1023666X.2021.2016305.

52 H. Bian, X. Shu, W. Su, D. Luo, M. Dong, X. Liu, X. Ji and H. Dai, Biodegradable, Flexible and Ultraviolet Blocking Nanocellulose Composite Film Incorporated with Lignin Nanoparticles, *Int. J. Mol. Sci.*, 2022, **23**(23), 14863, DOI: 10.3390/ijms232314863.

53 M. L. I. Montes, F. Luzi, F. Dominici, L. Torre, V. P. Cyras, L. B. Manfredi, D. Puglia and S. Farris, Design and Characterization of PLA Bilayer Films Containing Lignin and Cellulose Nanostructures in Combination With Umbelliferone as Active Ingredient, *Front. Chem.*, 2019, **7**, 1–13, DOI: 10.3389/fchem.2019.00157.

54 K. Jin, Y. Tang, X. Zhu and Y. Zhou, Polylactic Acid Based Biocomposite Films Reinforced with Silanized Nanocrystalline Cellulose, *Int. J. Biol. Macromol.*, 2020, **162**, 1109–1117.

55 M. J. Bof, A. Jiménez, D. E. Locaso, M. A. García and A. Chiralt, Grapefruit Seed Extract and Lemon Essential Oil as Active Agents in Corn Starch–Chitosan Blend Films, *Food Bioprocess Technol.*, 2016, **9**(12), 2033–2045, DOI: 10.1007/s11947-016-1789-8.

56 A. González and C. I. Alvarez Igarzabal, Soy Protein - Poly (Lactic Acid) Bilayer Films as Biodegradable Material for Active Food Packaging, *Food Hydrocolloids*, 2013, **33**(2), 289–296, DOI: 10.1016/j.foodhyd.2013.03.010.

57 S. Rizal, T. Alfatah, H. P. S. Abdul Khalil, E. B. Yahya, C. K. Abdullah, E. M. Mistar, I. Ikramullah, R. Kurniawan and R. D. Bairwan, Enhanced Functional Properties of Bioplastic Films Using Lignin Nanoparticles from Oil Palm-Processing Residue, *Polymers*, 2022, **14**(23), 1–20, DOI: 10.3390/polym14235126.

58 S. Roy and J. W. Rhim, Fabrication of Carboxymethyl Cellulose/Agar-Based Functional Films Hybridized with

Alizarin and Grapefruit Seed Extract, *ACS Appl. Bio Mater.*, 2021, **4**(5), 4470–4478, DOI: 10.1021/acsabm.1c00214.

59 R. Bhat, N. Abdullah, R. Hj and G. Tay, Producing Novel Sago Starch Based Food Packaging Films by Incorporating Lignin Isolated from Oil Palm Black Liquor Waste, *J. Food Eng.*, 2013, **119**(4), 707–713, DOI: 10.1016/j.jfoodeng.2013.06.043.

60 S. Wang, Y. Hao, Q. He and Q. Gao, Biodegradable Starch-Polyvinyl Alcohol Composite Films by the Incorporation of Lignin for Packaging Applications, *J. Thermoplast. Compos. Mater.*, 2024, **37**(11), 3413–3435, DOI: 10.1177/08927057241233566.

61 W. Yang, E. Fortunati, F. Dominici, G. Giovanale, A. Mazzaglia, G. M. Balestra, J. M. Kenny and D. Puglia, Effect of Cellulose and Lignin on Disintegration, Antimicrobial and Antioxidant Properties of PLA Active Films, *Int. J. Biol. Macromol.*, 2016, **89**, 360–368, DOI: 10.1016/j.ijbiomac.2016.04.068.

62 S. Roy and J.-W. Rhim, Agar-Based Antioxidant Composite Films Incorporated with Melanin Nanoparticles, *Food Hydrocolloids*, 2019, **94**, 391–398, DOI: 10.1016/j.foodhyd.2019.03.038.

63 Anushikha and K. K. Gaikwad, Lignin as a UV Blocking, Antioxidant, and Antimicrobial Agent for Food Packaging Applications, *Biomass Convers. Biorefin.*, 2024, **14**(15), 16755–16767, DOI: 10.1007/s13399-022-03707-3.

64 H. Mostafa, M. Hamdi, J. O. Airouyuwaa, F. Hamed, Y. Wang and S. Maqsood, Lignin and Green Solvent Extracted Phenolic Compounds from Date Palm Leaves as Functional Ingredients for the Formulation of Soy Protein Isolate Biocomposite Packaging Materials: A Circular Packaging Concept, *Int. J. Biol. Macromol.*, 2024, **279**, 134843, DOI: 10.1016/j.ijbiomac.2024.134843.

65 A. S. Koutoulis, A. E. Giannakas, D. G. Lazaridis, A. Kitsios, V. K. Karabagias, A. E. Giannakas, A. Ladavos and I. K. Karabagias, Preparation and Characterization of PLA-Based Films Fabricated with Different Citrus Species Peel Powder, *Coatings*, 2024, **14**(10), 1311, DOI: 10.3390/coatings14101311.

66 V. Ramya, S. Yamini, P. Siddappa, K. Murthy, D. Jeevan and P. Reddy, Synthesis of Lignin Nanoparticles Employing Acid Precipitation Method and Its Application to Enhance the Mechanical , UV-Barrier and Antioxidant Properties of Chitosan Films, *Int. J. Polym. Anal. Charact.*, 2022, **27**(2), 99–110, DOI: 10.1080/1023666X.2021.2016305.

67 M. Li, Y. Zhang, H. Ma, Q. Peng, D. Min, P. Zhang and L. Jiang, Improved Antioxidant Activity of Pretreated Lignin Nanoparticles: Evaluation and Self-Assembly, *Int. J. Biol. Macromol.*, 2024, **267**(P1), 131472, DOI: 10.1016/j.ijbiomac.2024.131472.

68 A. A. Oun and J. W. Rhim, Preparation of Multifunctional Carboxymethyl Cellulose-Based Films Incorporated with Chitin Nanocrystal and Grapefruit Seed Extract, *Int. J. Biol. Macromol.*, 2020, **152**, 1038–1046, DOI: 10.1016/j.ijbiomac.2019.10.191.

69 S. Roy and J. W. Rhim, Antioxidant and Antimicrobial Poly(Vinyl Alcohol)-Based Films Incorporated with Grapefruit Seed Extract and Curcumin, *J. Environ. Chem. Eng.*, 2021, **9**(1), 104694, DOI: 10.1016/j.jece.2020.104694.

70 H. Wei and M. A. Pascall, Evaluation of Structural and Functional Properties of Citrus Pectin Film Enriched with Green Tea Extract, *Polym. Eng. Sci.*, 2023, **63**(8), 2522–2533, DOI: 10.1002/pen.26393.

71 A. M. Tone, N. H. Solana, M. R. Khan, A. Borriello, E. Torrieri, C. S. Reig and F. M. M. Prieto, Study on the Properties of PLA- and PP-Based Films for Food Applications Incorporating Orange Peel Extract from Agricultural by-Products, *Polymers*, 2024, 1–26.

72 N. K. Alqahtani, B. Alkhamis, T. M. Alnemr and M. Mohammed, Combined Influences of Edible Coating and Storage Conditions on the Quality of Fresh Dates: An Investigation and Predictive Analysis Using Artificial Neural Networks, *Heliyon*, 2025, **11**(4), e42373, DOI: 10.1016/j.heliyon.2025.e42373.

73 B. Hu, L. Lin, Y. Fang, M. Zhou and X. Zhou, Application of Chitosan-Lignosulfonate Composite Coating Film in Grape Preservation and Study on the Difference in Metabolites in Fruit Wine, *Coatings*, 2022, **12**(4), 494.

74 H. Aloui, K. Khwaldia, L. Sánchez-González, L. Muneret, C. Jeandel, M. Hamdi and S. Desobry, Alginate Coatings Containing Grapefruit Essential Oil or Grapefruit Seed Extract for Grapes Preservation, *Int. J. Food Sci. Technol.*, 2014, **49**(4), 952–959, DOI: 10.1111/ijfs.12387.

75 E. Pereira, R. G. B. E Silva, W. A. Spagnol and V. Silveira Junior, Water Loss in Table Grapes: Model Development and Validation under Dynamic Storage Conditions, *Food Sci. Technol.*, 2018, **38**(3), 473–479, DOI: 10.1590/1678-457x.08817.

76 Q. Feng, C. Zhu, P. Zhou, J. Yao, Y. Bao and Z. Zhao, Effects of ε-Polylysine Combined with Plant Extract on the Microbiological and Sensory Qualities of Grapes, *Foods*, 2025, **14**(3), 516, DOI: 10.3390/foods14030516.

77 Z. Zhu, J. Liang, C. Zhou, K. Huang, X. Fan, M. Zhou, B. Xu, C. Huang, H. Li, H. Ma and L. Chen, Synergistic Enhancement of Gelatin-Chitosan Films with Vanillin Schiff Base and ZnO for Effective Strawberry Preservation, *Food Control*, 2025, **180**, 111647, DOI: 10.1016/j.foodcont.2025.111647.

78 H. Chang, K. Li, J. Ye, J. Chen and J. Zhang, Effect of Dual-Modified Tapioca Starch/Chitosan/SiO2 Coating Loaded with Clove Essential Oil Nanoemulsion on Postharvest Quality of Green Grapes, *Foods*, 2024, **13**(23), 3735, DOI: 10.3390/foods13233735.

79 X. Wu, H. Wang, Y. Zhou, W. Xi, Y. Zhang, S. Li, J. Tang, S. Li, Q. Zhang, Y. Liu, J. Li, M. Chen and W. Qin, Preservation of Anthocyanins in Postharvest Grapes Through Carboxymethyl Chitosan Films Containing Citrus Essential Oil Emulsion via Enzymatic Regulation, *Foods*, 2025, **14**(12), 1–21, DOI: 10.3390/foods14122015.

80 H. Du and L. He, Synergistic Improvement of Antioxidant and Antibacterial Properties of Carbon Quantum Complexes with Zinc Doping and Chlorogenic Acid for Longan Preservation, *Food Chem.*, 2024, **439**, 138169, DOI: 10.1016/j.foodchem.2023.138169.